The Cryosphere Discussions

Snow depth in high-resolution regional climate model simulations over southern Germany - suitable for extremes and impact-related research?

Benjamin Poschlod[1], Anne Sophie Daloz[2]

[1]Research Unit Sustainability and Climate Risk, Center for Earth System Research and Sustainability (CEN), Universität Hamburg, 20144 Hamburg, Germany
[2]Center for International Climate Research (CICERO), 0349 Oslo, Norway

Correspondence to: Benjamin Poschlod (benjamin.poschlod@uni-hamburg.de)

Abstract. Snow dynamics play a critical role in the climate system as they affect the water cycle, ecosystems and society. Within climate modelling, the representation of the amount and extent of snow on the land surface is crucial for simulating the mass and energy balance of the climate system. Here, we evaluate simulations of daily snow depths against 83 station observations in southern Germany over the time period 1987 – 2018. Two simulations stem from high-resolution regional climate models, the Weather Research & Forecasting Model (WRF) at 1.5 km resolution and the COSMO-CLM (CCLM) at 3 km resolution. Additionally, the hydrometeorological snow model AMUNDSEN is run at the point scale of the climate stations based on the atmospheric output of CCLM. The ERA5-Land dataset (9 km) complements the comparison as state-of-the-art reanalysis land surface product. All four simulations are driven by the same atmospheric boundary conditions of ERA5. The WRF simulation features a cold bias of -1.2°C and slightly overestimates snow depth (+0.4 cm) with a root-mean-square error (RMSE) of 4.3 cm. Snow cover duration slightly exceeds the observations (+6.8 d; RMSE = 20.5 d). The CCLM reproduces the winter climate very well, but shows a strong negative bias at snow depth (-2.5 cm; RMSE = 5.6 cm) and snow cover duration (-20.0 d; RMSE = 27.1 d). AMUNDSEN improves the reproduction of snow cover duration (+6.5 d; RMSE = 16.6 d) and snow depth (+2.2 cm; RMSE = 6.2 cm). ERA5-Land shows a strong positive bias in mean winter snow depth (+3.6 cm; RMSE = 14.5 cm) and snow cover duration (+33.9 d; RMSE = 44.0 d). All models fail to skilfully predict white Christmas.

For extreme events of snow dynamics such as annual maximum snow depths, maximum daily snow accumulation and melting, the ERA5L and CCLM show large biases in amplitude and deviations in seasonality. WRF and AMUNDSEN can improve the representation of extremes but still with considerable limitations.

The high spatial resolution of convection-permitting climate models shows potential in reproducing the winter climate in southern Germany. However, the uncertainties within the snow modelling prevent a further straightforward use for impact research. Hence, careful evaluation is needed before any impact-related interpretation of the simulations, also in the context of climate change research.

1 Introduction

30

The presence and absence of snow, as well as snow depth, affect nature and humans on many different levels. The albedo of snow influences the radiation and energy balance of the surface (Warren, 2019). Its insulating effect protects plants and animals (Blume-Werry et al., 2016; Slatyer et al., 2022). In addition, snow cover affects the microbial structure of the soil (Gavazov et al., 2017). The seasonal cycle of snow cover duration and snow depth governs soil moisture dynamics (Qi et al., 2020) and

35 also the runoff regime of rivers and streams (Girons Lopez et al., 2020; Poschlod et al., 2020a). Hence, the snow dynamics also affect the freshwater availability in large regions of the world (Barnett et al., 2005). Snow melt may also induce riverine floods (Berghuijs et al., 2019), often in combination with heavy rainfall (Poschlod et al., 2020b). Sufficient snow depths are needed for ski tourism (Steiger et al., 2017; Witting and Schmude, 2019), but also expected by non-ski tourists during their winter holidays in the mountains (Bausch and Unseld, 2018). This reflects also a traditional and cultural meaning of snow

40 cover, which manifests annually in discussions and expectations about "white Christmas" in the Northern Hemisphere (Durre and Squires, 2015; Harley, 2003). Moreover, the presence of snow influences everyday life in terms of mobility. Usage of bikes or scooters is reported to significantly depend on snow depths (Mathew et al., 2019; Yang et al., 2018). Also, the alternatives (trains, cars, planes) may be affected by high snow depths (Doll et al., 2014; Taszarek et al., 2020; Trinks et al., 2012). During extreme snow events, power shortages (Bednorz, 2013; Gerhold et al., 2019) or even collapses of roofs (Strasser,

45 2008a) occur, which is why building codes have to rely on the regional snow climate (Croce et al., 2018).

Due to these manifold effects, there is great interest in modelling snow dynamics and snow depths in order to be able to predict near-term snow conditions (Hammer, 2018) and to project future snow conditions (Frei et al., 2018). Snow models in general are used to simulate snow dynamics on different temporal and spatial scales. In global or regional earth system model setups, snow dynamics are simulated coupled with atmospheric processes and other land surface processes (Krinner et al., 2018).

50 However, the spatial resolution of global and regional models is often not sufficient to represent complex terrain and the spatial variability of the land surface (Mooney et al., 2022). Further, the simulated climate and snow dynamics show biases (Daloz et al. 2022). Often, for local to regional impact studies, the climatic biases are adjusted, where it is necessary to apply a method tailored to snow climates (e.g. Chen et al., 2018; Frei et al., 2018; Meyer et al., 2019). In the case of a simple univariate bias adjustment, the dependence between temperature and precipitation is not considered, which neglects the threshold effect of air

55 temperature on fractionation of precipitation into rain and snowfall (Meyer et al., 2019). Therefore, multivariate bias adjustment is recommended for hydrological impact modelling in regions with snow and rain dynamics (Chen et al., 2018; Meyer et al., 2019). In a next step, snow models are set up at higher resolution, driven by bias-adjusted climatic time series (Hanzer et al., 2018). However, then the simulated snow dynamics cannot feed back into the climate, which is why these simulations are called "offline". Another possibility would be to directly adjust the biases of the snow parameter simulated by

60 the climate model (Matiu and Hanzer, 2022).

Due to the advances in computational power, the spatial resolution of regional climate models (RCMs) has increased (Coppola et al., 2020). Kilometre-scale simulations are available for decade-long time spans. The high spatial resolution allows for a

finer-scale representation of complex topography (Poschlod et al., 2018). Therefore, the effects of altitude on air temperature can be mapped in more detail, which better represents the fractionation into rain and snowfall, as well as melting and

65   accumulation processes. In addition, the higher resolution of land cover allows for more detailed simulation of the albedo, which in turn governs the energy balance (Winter et al., 2017). Future work aims at even implementing snow drift due to wind and turbulence (Saigger et al., 2023).

Here, two high-resolution convection-permitting regional climate models are evaluated with station observations of daily snow depth in southern Germany for a 31-year period within 1987 – 2018. We analyse simulations of the Weather Research and

70   Forecasting (WRF) model (Skamarock et al., 2019) at 1.5 km resolution and the COnsortium for Small scale MOdelling (COSMO; Sørland et al., 2021) model in climate mode (CLM) at 3 km resolution (hereafter abbreviated to CCLM). Both models are driven by atmospheric boundary conditions of ERA5 (Hersbach et al., 2020) at 31 km resolution. Moreover, the hydrometeorological snow model AMUNDSEN is run at the point scale of the climate stations driven by the atmospheric output of CCLM. In addition, the state-of-the-art land surface reanalysis product ERA5-Land (9 km resolution; Muñoz-Sabater

75   et al., 2021) is compared.

Such evaluation is important as future projections of snow dynamics are often based on regional climate models (e.g. Frei et al., 2018; Räisänen, 2021). Even if mean snow depth and mean snow cover duration are expected to decrease due to higher temperatures, risks associated with snow dynamics might not (Musselman et al., 2018). While there are studies on climate model simulations and extreme snowfall (Quante et al., 2021; Sasai et al., 2019), we find less literature about extremes of snow

80   depth dynamics within climate model simulations. Furthermore, there are studies evaluating regional climate models based on multi-decadal simulations (Daloz et al., 2022; Matiu and Hanzer, 2022), however at coarser spatial resolution (0.11°). Hence, we see the need for a critical examination of what current state-of-the-art high-resolution RCMs are capable of in terms of snow dynamics and extremes.

2 Data and methodology

85   A comparative overview of the investigated simulation data is given in Table 1. The following sections describe the different model features and setups in detail. As a preliminary remark, we would like to point out that the historical genesis of the different model setups still governs the degree of complexity of the snow schemes. Single-layer snow schemes are common in the atmospheric community for numerical weather prediction (NWP) models and reanalyses (Arduini et al., 2019).

90   **Table 1: Overview of the different investigated model setups.**

Boundary conditions	Downscaling	Spatial resolution	Land surface / snow model	maximal number of snow layers	Range of snow albedo

ERA5 (Hersbach et al., 2020)	Statistical: ERA5-Land Muñoz-Sabater et al. (2021)	9 km	CHTESSEL (ECMWF, 2018)	1	exposed: 0.5 to 0.85; forested: 0.27 to 0.38
ERA5 (Hersbach et al., 2020)	Dynamical: COSMO-CLM (Doms et al., 2021)	3 km	TERRA-ML (Doms et al., 2021)	1	exposed: 0.4 to 0.7; forested: empirical reduction factor
ERA5 (Hersbach et al., 2020)	Dynamical: COSMO-CLM (Doms et al., 2021)	3 km	AMUNDSEN (Strasser, 2008b; Hanzer et al., 2018)	3	exposed: 0.55 to 0.85
ERA5 (Hersbach et al., 2020)	Dynamical: WRF (Skamarock et al., 2019)	1.5 km	NOAH_MP (Niu et al., 2011)	3	exposed, non-melting: 0.7 to 0.84; exposed, melting: 0.5 to 0.84; forested: see Niu and Yang (2004)

2.1 Regional climate models

Both RCMs are driven by atmospheric boundary conditions of the ERA5 reanalysis at 31 km resolution. The WRF simulations have been carried out by Collier and Mölg (2020), where the setup is described in detail. The WRF is run in version 4.1

95 (Skamarock et al., 2019). The boundary conditions by ERA5 drive the WRF at 7.5×7.5 km² (one-way nesting), where spectral nudging is applied. The forcing at the lateral boundaries is updated at 3-hourly steps. Increasing the spatial resolution by factor five within a second nesting step results in simulations at 1.5×1.5 km² resolution, where convective processes are explicitly resolved. Collier and Mölg (2020) provide a general climatic evaluation with observational data. In order to simulate surface processes WRF is run coupled with the land surface scheme NOAH_MP (Niu et al., 2011). The physically-based snow model

100 in NOAH_MP features up to three snow layers, which are divided based on the simulated snow depth. In addition, four soil levels and a vegetation canopy layer are considered. Interception and burial of vegetation by snow is modelled following Niu and Yang (2004). Based on the energy balance for the snow and soil layers, the temperatures of the layers are calculated. For above/below 0°C, melting and freezing are assumed. Mass and energy transfer between layers is accounted for (Niu et al., 2011). In order to derive the snow depth, the density is assessed representing snow metamorphism and compaction following

105 Anderson (1976) and Sun et al. (1999). The snow surface albedo is calculated following the CLASS scheme (Verseghy, 1991), where the albedo of fresh snow is assumed to amount to 0.84. During melting conditions, the albedo exponentially decreases

with 0.5 as lower limit. Without melting conditions, 0.7 is assumed as lower limit. The snow albedo of forested areas is modelled dependent on the leaf and stem area index accounting for snow interception, loading and unloading of snow as well as melting and refreezing (Niu and Yang, 2004). The ground surface albedo is calculated as an area-weighted average of the snow albedo and bare soil albedo (Niu et al., 2011). The WRF data are openly available (Collier, 2020).

COSMO was operationally applied as weather forecasting model in Germany over 20 years being replaced by ICON (Rybka et al., 2022). For regional climate simulations, the ICON-CLM is developed (Pham et al., 2021). Here, still the CCLM version 5-0-16 at 3 km resolution (Brienen et al., 2022) is directly driven by the atmospheric conditions from ERA5, where the forcing is updated every hour (Rybka et al., 2022). The simulation domain covers Germany, surrounding catchments and parts of the Alps. Hence, the analysis domain is well within the simulation domain. The 3 km resolution allows for explicit simulation of deep convection, whereby shallow convection is parametrized. The land surface model TERRA_ML is implemented in COSMO-CLM and represents soil, vegetation and snow dynamics (Doms et al., 2021, Schulz and Vogel, 2020). It features multiple soil layers and either one interception reservoir or one snow reservoir on top of the soil, depending on the predicted temperature of the stored water. However, no canopy layer is implemented, which is common in NWP models, but represents a strong simplification for climate models (Schulz et al., 2016). Mass and energy fluxes between the atmosphere, the interception/snow reservoir and the soil layers govern the temperature of the water in the reservoir. In case of snow cover, the mean snow temperature is calculated based on the heat capacity of the snow, the atmospheric forcing at the snow surface, the heat flux to the soil, and melting processes (Doms et al., 2021). The prediction of snow density includes two processes. Aging increases the mean snow density of the reservoir, whereas newly fallen snow decreases the mean density. The range of densities is fixed between 50 and 400 kg/m³. Doms et al. (2021) claim that extreme snow depths cannot be properly accounted for by the model concept. The range of possible snow depths is restricted between 0.01 to 1.5 m. A time-dependent snow surface albedo is calculated, where the albedo covers the range between 0.4 for old snow and 0.7 for fresh snow (Doms et al., 2021). As the model features no canopy layer, no shading effects of vegetation are simulated. Instead an empirical reduction factor for the snow albedo under vegetation is applied (Daloz et al., 2022). The CCLM data are available publicly (see https://esgf.dwd.de/projects/dwd-cps/). However, albedo data were provided separately without quality checks (pers. comm. Susanne Brienen, German Weather Service).

2.2 Land surface model in ERA5-Land

ERA5-Land (ERA5L) directly derives its atmospheric forcing from the 10 m level of ERA5 at hourly resolution (Muñoz-Sabater et al., 2021). The 31 km resolution of ERA5 is linearly interpolated on the 9 km grid of ERA5-Land. The land surface model Carbon Hydrology-Tiled ECMWF Scheme for Surface Exchanges over Land (CHTESSEL) then simulates energy and water cycles globally over land at hourly resolution. The snow scheme features one layer with a single temperature and density on top of the four-layer soil (ECMWF, 2018). The snow temperature is calculated based on the energy fluxes between the atmosphere and the snow skin, melting processes, and basal heat flux. Snow temperature, mass, and density are used to derive the liquid water content within the snow pack. Interception of liquid water by the snow pack is accounted for. The snow density

140   is assumed to change due to overburden, thermal metamorphisms (Anderson, 1976) and compaction (Lynch-Stieglitz, 1994).
The range of snow densities is restricted between 50 and 450 kg/m³. The calculation of the snow surface albedo for exposed
areas follows Verseghy (1991) with values between 0.5 and 0.85. For forested areas, lower albedo values between 0.27 and
0.38 are applied following Moody et al. (2007) who based their calculations on remote sensing products from MODIS. Further
details of the land surface scheme are provided by ECMWF (2018) and especially for the snow scheme by Dutra et al. (2010).

145   The ERA5L data are openly available (https://cds.climate.copernicus.eu/cdsapp#!/dataset/reanalysis-era5-land?tab=overview). For the next land surface model generation, Bousetta et al. (2021) present the new ECLand model, which
introduces a multi-layer snow scheme following Arduini et al. (2019).

2.3 Hydroclimatological model AMUNDSEN

The hydroclimatological model AMUNDSEN has been developed to dynamically resolve the mass and energy balance of

150   snow and ice in high-mountain regions (Strasser, 2008b; Hanzer et al., 2018). The model can be set up spatially distributed at
high resolution (e.g. 10 m to 100 m) and includes snow redistribution processes and a radiation scheme accounting for e.g.
terrain slope and hill shading (Hanzer et al., 2016). Here, we apply the model at point scale at the locations of the 83 climate
stations. We use the CCLM output of hourly temperature, precipitation, wind speed, relative humidity and shortwave radiation
to drive openAMUNDSEN, the open model version implemented in Python (Warscher et al., 2021). No model-internal

155   correction for precipitation undercatch is applied as the climatological input stems from simulated precipitation by the CCLM.
AMUNDSEN uses the wet-bulb temperature to differentiate between solid and liquid precipitation (Hanzer et al., 2018). The
model features three snow layer categories, which are named "new snow", "old snow", and "firn", depending on the snow
density and age. The snow density is calculated following Anderson (1976) and Jordan (1991) considering compaction and
metamorphism. Snow with a density above 200 kg/m³ is transferred to the old snow layer. The firn layer does not apply for

160   the 83 locations as no multi-year snow cover is simulated. Melting water in the snowpack may be retained applying a
parametrization by Braun (1984). Snow albedo is parametrized depending on the age of the snow in a range between 0.55 and
0.85 for exposed surfaces following Hanzer et al. (2016). Snow-free albedo is set to 0.23 representing grassland according to
the climate station conditions.

2.4 Study area and observational data

165   The study area covers large parts of southern Germany, where the boundaries are given by the smallest simulation domain of
the WRF model and the national borders. It includes a wide range of elevations between roughly 100 m and 3000 m above sea
level (see Fig. 1a) with therefore different snow dynamics. For the comparison to snow depth observations, we select 83 climate
stations with less than 30 % missing data, which are operated by the German Weather Service (DWD, 2023). In order to assess
the climatology, temperature and precipitation is analysed as well, where precipitation is not corrected for undercatch. The

170   mean annual temperatures of the locations range from 5.4 °C to 10.9 °C and the mean annual precipitation covers the range
between 580 mm and 1700 mm. The analysis period spans from November 1987 to April 2018 yielding 31 extended winter

seasons. In this study, the extended winter season is defined as six-month period from November to April. All analysis is carried out at daily resolution.

The comparison between measured snow depth at the climate station and the simulated gridded snow depth is carried out via
175 nearest-neighbour approach. As the elevation within the gridded models differs according to the spatial resolution (Fig. 1b-d; see also Fig. S1), the elevation of the climate station and the nearest model grid cell may deviate. Figure 2 shows to what degree the finer spatial resolution improves the representation of the altitude. The mean absolute deviation amounts to 24 m (WRF), 42 m (CCLM), and 93 m (ERA5L).
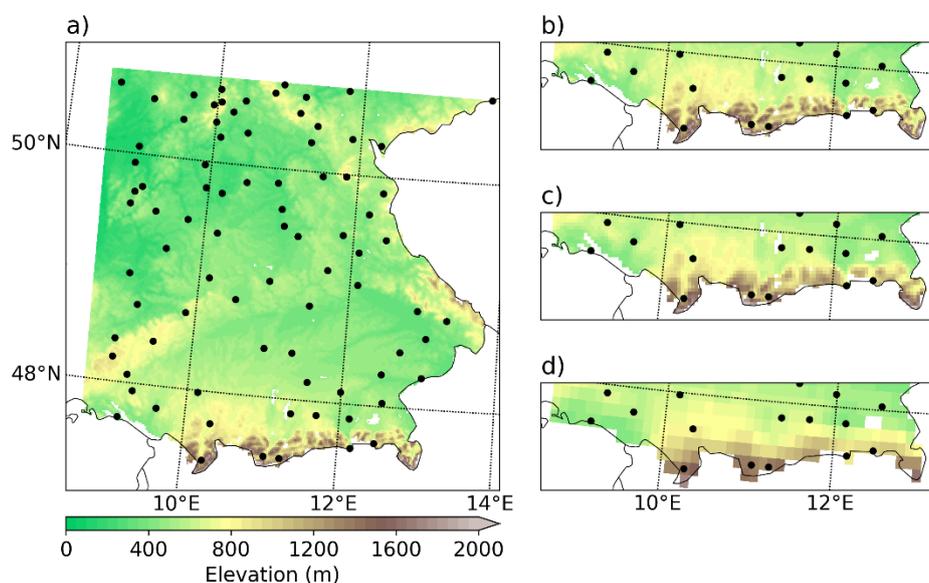
180 **Figure 1: Representation of elevation in the WRF (a). Lakes are masked out. The black dots show the 83 climate stations, where snow depth is observed. Zoomed display of the complex terrain in the southern study area in WRF (b), CCLM (c), and ERA5-Land (d).**
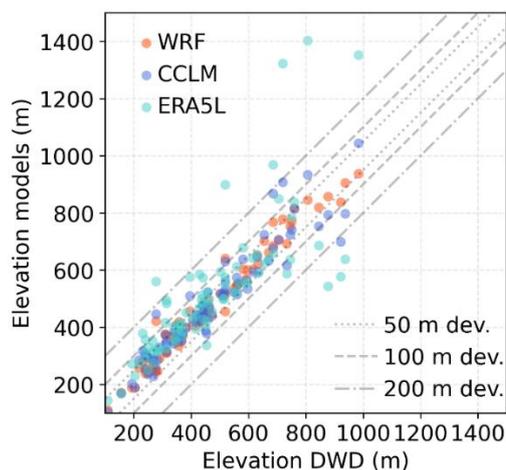
Figure 2: Comparison of the climate station elevation and the model elevation.

2.5 Evaluation criteria

We evaluate the RCMs at the 83 climate stations and calculate the deviations for each winter season. The performance is assessed with four measures, the mean absolute error (MAE), the root-mean-square error (RMSE), the bias (BIAS) or percentage bias (PBIAS), and Pearson rank correlation (r). For n observed values x_{obs} and simulated values x_{sim}, the measures are defined as follows:

$$MAE = \frac{\sum_{i=1}^{n} |x_{obs,i} - x_{sim,i}|}{n}, \tag{1}$$

$$RMSE = \sqrt{\frac{\sum_{i=1}^{n} (x_{obs,i} - x_{sim,i})^2}{n}}, \tag{2}$$

$$BIAS = \frac{\sum_{i=1}^{n} x_{sim,i} - x_{obs,i}}{n}, \tag{3}$$

$$PBIAS = \frac{\sum_{i=1}^{n} x_{sim,i} - x_{obs,i}}{\sum_{i=1}^{n} x_{obs,i}} \cdot 100, \tag{4}$$

$$r = \frac{\sum_{i=0}^{n} (x_{obs,i} - \bar{x}_{obs})(x_{sim,i} - \bar{x}_{sim})}{\sqrt{\sum_{i=1}^{n} (x_{obs,i} - \bar{x}_{obs})^2 \sum_{i=1}^{n} (x_{sim,i} - \bar{x}_{sim})^2}}, \tag{5}$$

In addition, we evaluate the simulations regarding intensity and time-related measures of snow dynamics. Thereby, mean winter snow depth refers to the mean snow depth over November to April. We define the snow cover duration as the number of days with more than 0.01 m snow depth considering the whole year. White Christmas is defined as more than 0.01 m snow depth on the 24th, 25th, and 26th of December following the German Weather Service (DWD 2020).

In order to assess extreme conditions, we sample the annual maxima of snow depth. Based on this sampling, we fit the Generalized Extreme Value (GEV) distribution, which can be applied to derive return levels of snow depth, where

$$GEV(x; \xi) = \begin{cases} \exp\left(-\left[1 + \xi\left(\frac{x-\mu}{\sigma}\right)\right]^{-1/\xi}\right), \xi \neq 0 \\ \exp\left(-\exp\left(-\frac{x-\mu}{\sigma}\right)\right), \xi = 0, \end{cases} \quad x \in \mathbb{R}, \tag{6}$$

for parameters μ (location), σ (scale) and ξ (shape). The location parameter governs the centre of the distribution, the scale parameter corresponds to its spread, whereas the shape parameter governs the tail behaviour (Coles, 2001). We estimate these GEV parameters using a Markov Chain Monte Carlo algorithm (Bocharov, 2022; Foreman-Mackey et al., 2013) also generating confidence intervals at the 95 % level.

210 Furthermore, extreme daily snow accumulations and melting are investigated. These two variables are derived from the daily change in snow depth. Hence, for the daily maxima of snow depth reduction, snow melt (and not compaction) is simplifying assumed as main driving process.

3 Model evaluation

3.1 Biases of winter air temperature and precipitation

215 Precipitation and air temperature govern the snow dynamics to a large degree. The comparison of simulated and observed winter temperature and precipitation is shown in Figure 3. The WRF systematically simulates too low winter temperature, which has already been noted by Collier and Mölg (2020). Winter temperature is closely reproduced by the CCLM with no bias (Fig. 3b). ERA5L has a slight cold bias, mostly due to single stations, where the underestimation amounts to 4°C (see Fig. 3c) resulting from the elevation bias (Fig. 2). The WRF model slightly underestimates winter precipitation. However, as we

220 do not correct the observed precipitation for undercatch, we would expect a slight overestimation of the RCMs. The CCLM can reproduce winter precipitation with smaller errors, where the positive percentage bias of 9.5 % falls in the range of possible undercatch-induced deviations in southern Germany (Richter, 1995). The coarser resolved ERA5L shows the biggest deviations with a stronger positive deviation and lowest rank correlation.

The differences of the station elevation and the mean grid cell altitude also contribute to these biases. Elevation governs the

225 temperature and also orographic precipitation effects (Warscher et al., 2019). Hence, Figures 4a-c provide a comparison of the mean 31-year bias per location and the elevation difference. The Pearson rank correlations between elevation (bias) and temperature or precipitation bias are given in Table 2. For the biases of ERA5L, the relationship is clearly visible (Fig. 4c), where higher (lower) elevation bias leads to over- (under)estimation of precipitation ($r = 0.49$) and under- (over)estimation of temperature ($r = -0.88$). For WRF and CCLM, no strong correlation is found, only a weak correlation of $r = 0.22$ for the
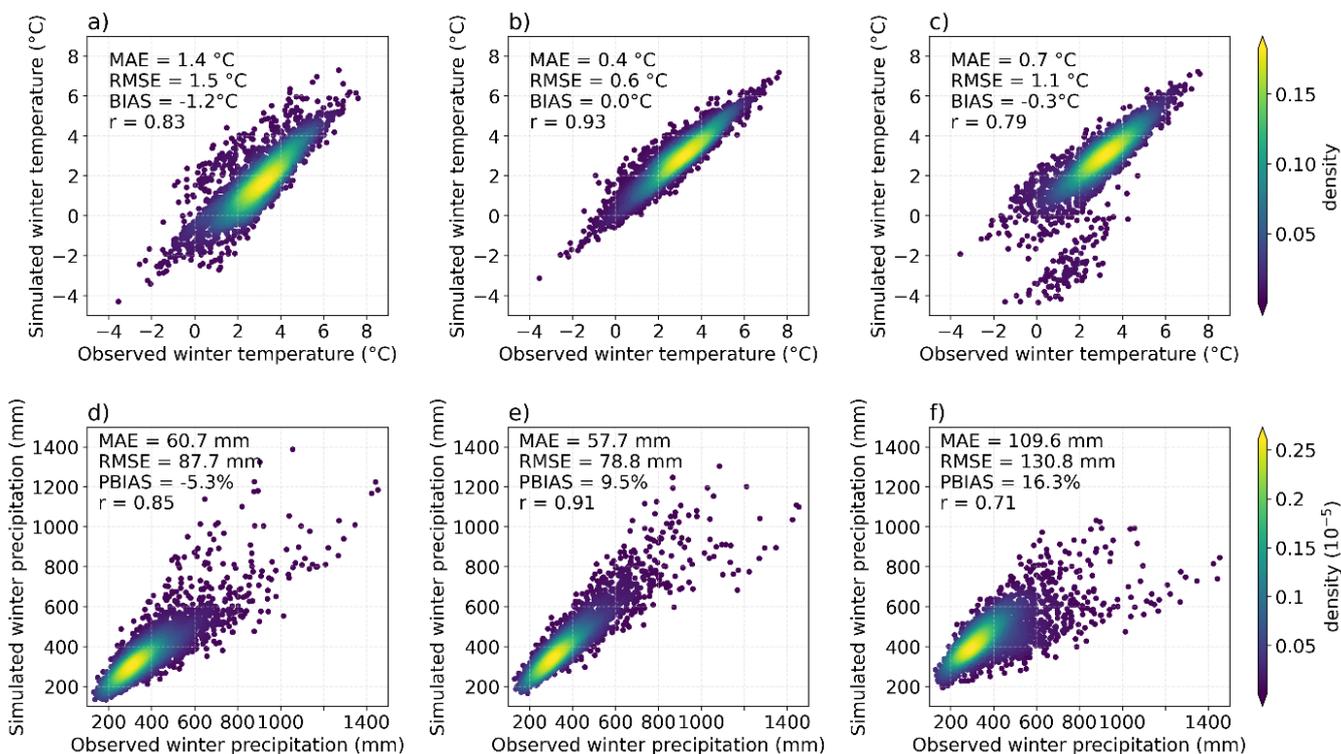
230 temperature bias in WRF.

Figure 3: Mean winter temperature (a-c) and precipitation (d-f) for each winter season and location in 1987 – 2018. Simulations by the WRF model (a,d), CCLM (b,e), and ERA5L (c,f) are compared to observations.

235

Table 2: Pearson rank correlation for elevation and climatological biases. Significant correlations at the 95 % (99 %) level are marked with one (two) asterisks.

Rank correlation between…	WRF	CCLM	ERA5L
Elevation bias and temperature bias	0.22*	0.00	-0.88**
Elevation bias and precipitation bias	-0.03	-0.18	0.49**
Model elevation and temperature bias	0.60**	0.50**	-0.58**
Model elevation and precipitation bias	0.05	0.32**	-0.10
Station elevation and temperature bias	0.55**	0.48**	-0.03
Station elevation and precipitation bias	0.05	0.37**	-0.47**

240 However, when comparing the absolute model elevation of each location, the CCLM shows systematic deviations (Fig. 4e). Locations at higher (lower) model elevation tend to have too high (low) temperatures (r = 0.50) and to be too wet (dry; r =

10

0.32). The WRF shows higher temperature biases for higher elevations (Fig. 4d) yielding an overall rank correlation of r = 0.60. The negative correlation between ERA5L model elevation and temperature bias (r = -0.58) is governed by the locations at high elevation (see Fig. 4f upper left corner) and medium-high elevation (see Fig. 4f lower right corner), as their temperature
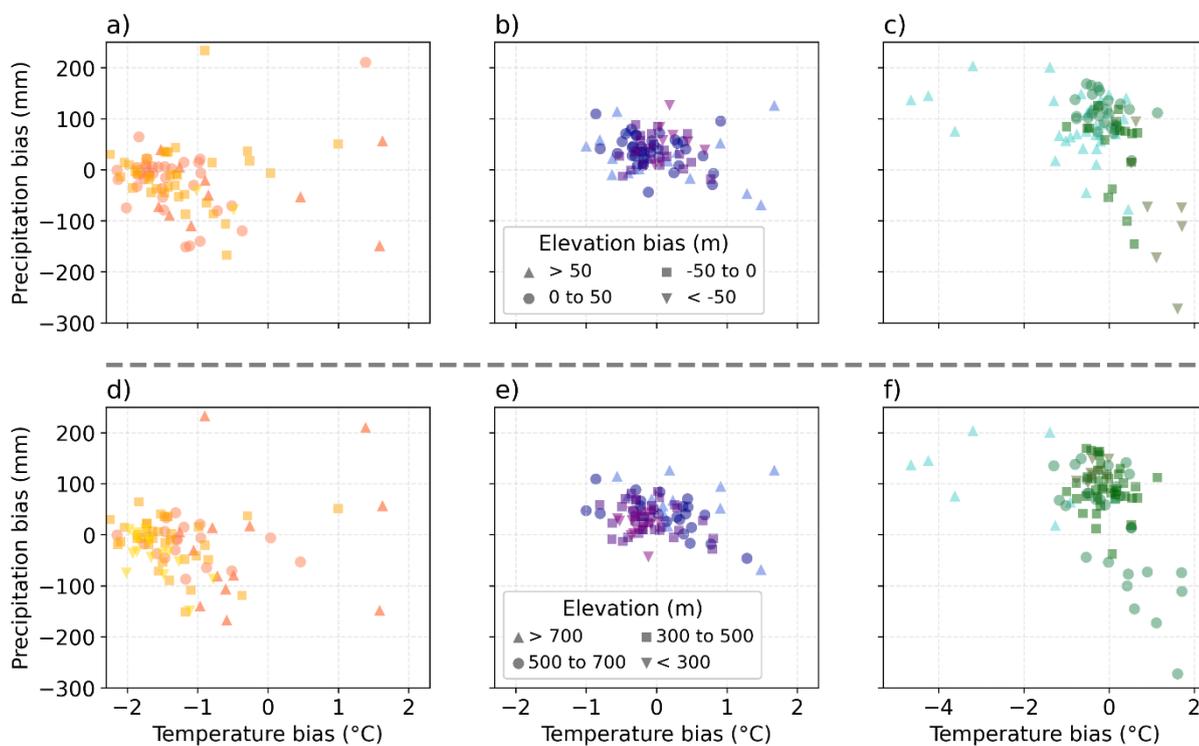245 bias results from the high elevation bias (see Figs. 2 and 4c).

Figure 4: Mean winter temperature and precipitation biases for each location averaged over 1987 – 2018 for simulations by the WRF model (a,d), CCLM (b,e), and ERA5L (c,f). The markers in the upper row (a-c) refer to the elevation bias between model and
250 **station. The markers in the lower row (d-f) show the absolute elevation of the respective model.**

3.2 Snow depth evaluation

The evaluation of snow depth time series is challenging due to the high memory of the system and error propagation over time. Furthermore, a proper evaluation depends on the intended use of the model data. If, for example, snow depth is simulated differently to an observation on the first day, but then correctly no change in snow depth is calculated for weeks, the error of
255 the first day propagates for weeks, although the model only simulated the accumulation differently on the first day.
To visualize this behaviour, we present the temporal evolution of snow depth during the winter season 2005/2006 at five selected locations (Fig. 5). In this season, continuous snow cover with several freezing and thawing cycles caused roof

The Cryosphere
Discussions

collapses and building evacuations in Bavaria (Strasser, 2008a). The time series show the temporal variability, the propagation
of deviations, and the variability between models.

260   In the further evaluation, 31 of these time series for 83 locations are condensed into different evaluation measures. We try to
evaluate the simulations based on different impact-relevant measures.
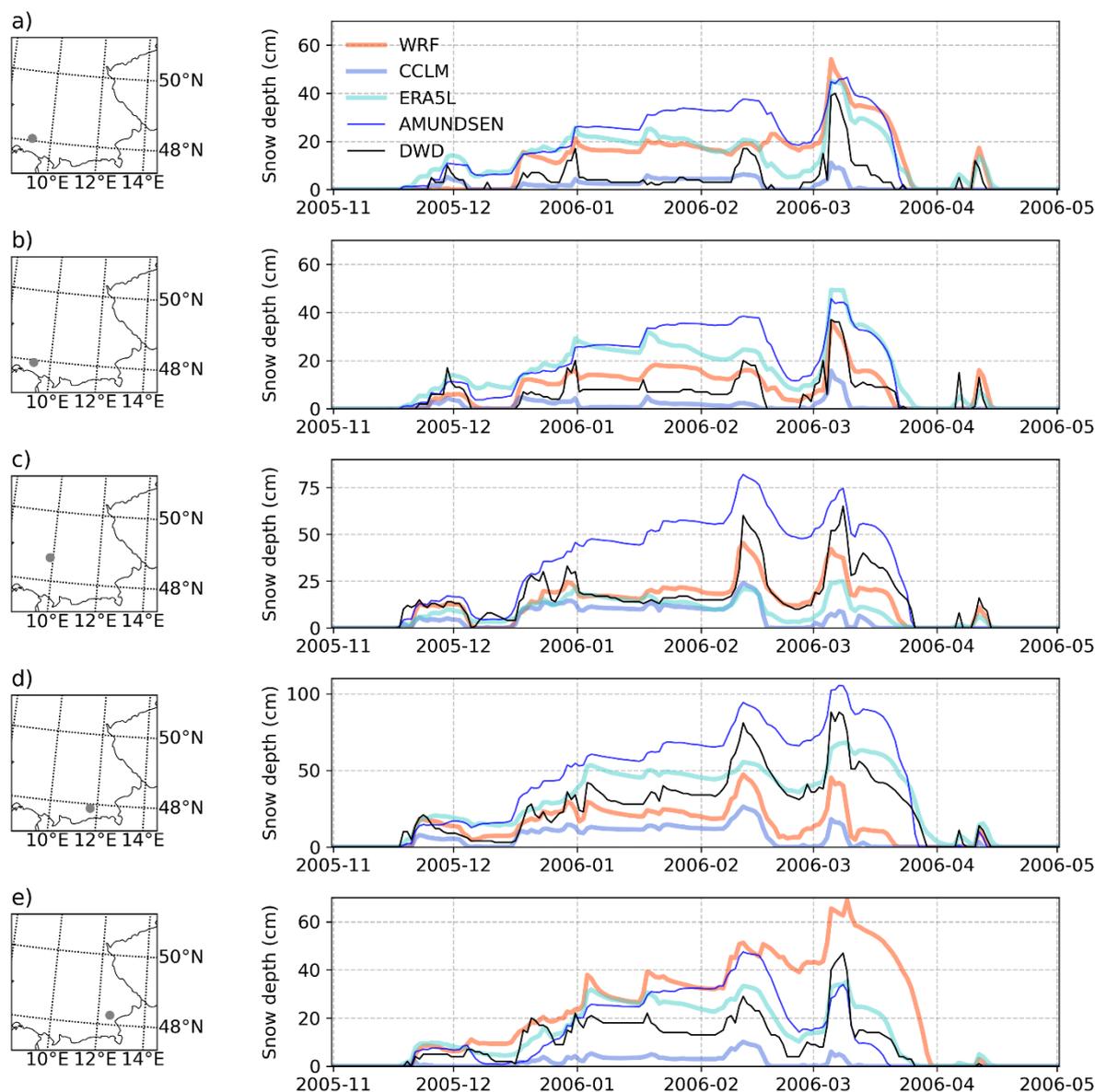
265   **Figure 5: Observed and simulated daily snow depth over the winter season 2005/2006 at five locations.**

The mean snow depth over the 31 winter half years in 1987 – 2018 varies largely between the models (Fig. 6). The deviations to the climate stations are minor in the flat areas with generally less snow depth. WRF, ERA5L, and AMUNDSEN slightly overestimate snow depth in the flat areas, while CCLM slightly underestimates. In the northern topographically complex

270   regions of the middle mountain range Ore Mountains (far north-east), Thuringian Forest (north central) and Rhön (north at 10°E), WRF, CCLM, and ERA5L underestimate (red dots in the north in Fig. 6a-c), whereas AMUNDSEN overestimates snow depth. In the Alps, ERA5L largely overpredicts the snow depths, whereas CCLM underestimates heavily. WRF underestimates to a moderate degree and AMUNDSEN shows almost no bias. A general overview of simulated and observed snow depths against the elevation is provided in Figure S2.

275
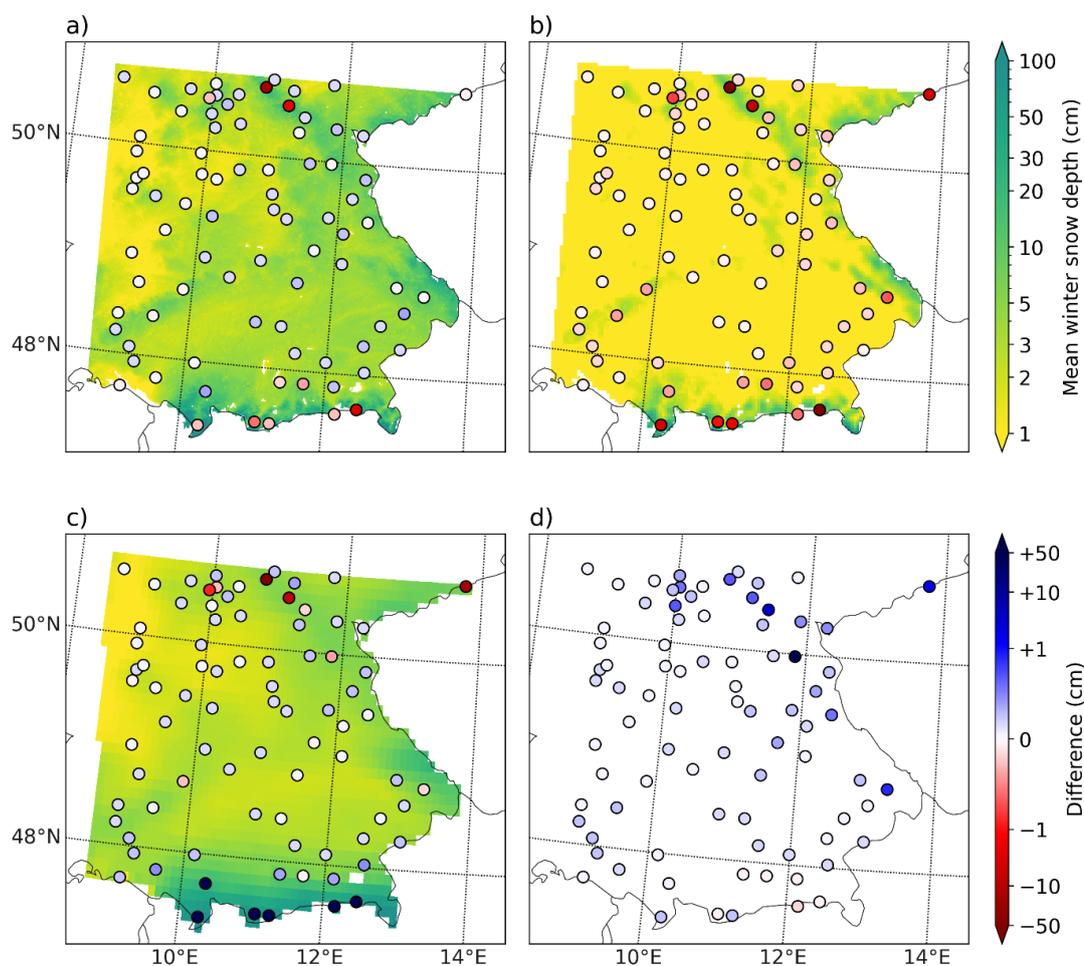
Figure 6: Mean winter snow depth 1987 – 2018 simulated by the WRF model (a), CCLM (b), ERA5L (c), and AMUNDSEN (d). The differences at the stations (coloured dots) are calculated as model minus observation. Red (blue) colour refers to an under- (over)estimation of the model. Note the logarithmic colour scaling.

280

The Cryosphere
Discussions

Open Access

EGU

When assessing mean winter snow depth separately for each season and location, the WRF model shows the lowest bias and errors (Fig. 7a). The systematic negative bias of the CCLM manifests itself in the fact that an overestimation of snow depth is simulated for almost no station at any season (Fig. 7b; the magnitude of the bias is equal to the MAE). The ERA5L simulations have the highest bias and errors, with high snow depth calculated for some low snow depth seasons and vice versa (upper left

285 and lower right of Fig. 7c). AMUNDSEN shows the best rank correlation and the best reproduction of observed high snow depth seasons, however with a tendency to overestimate.
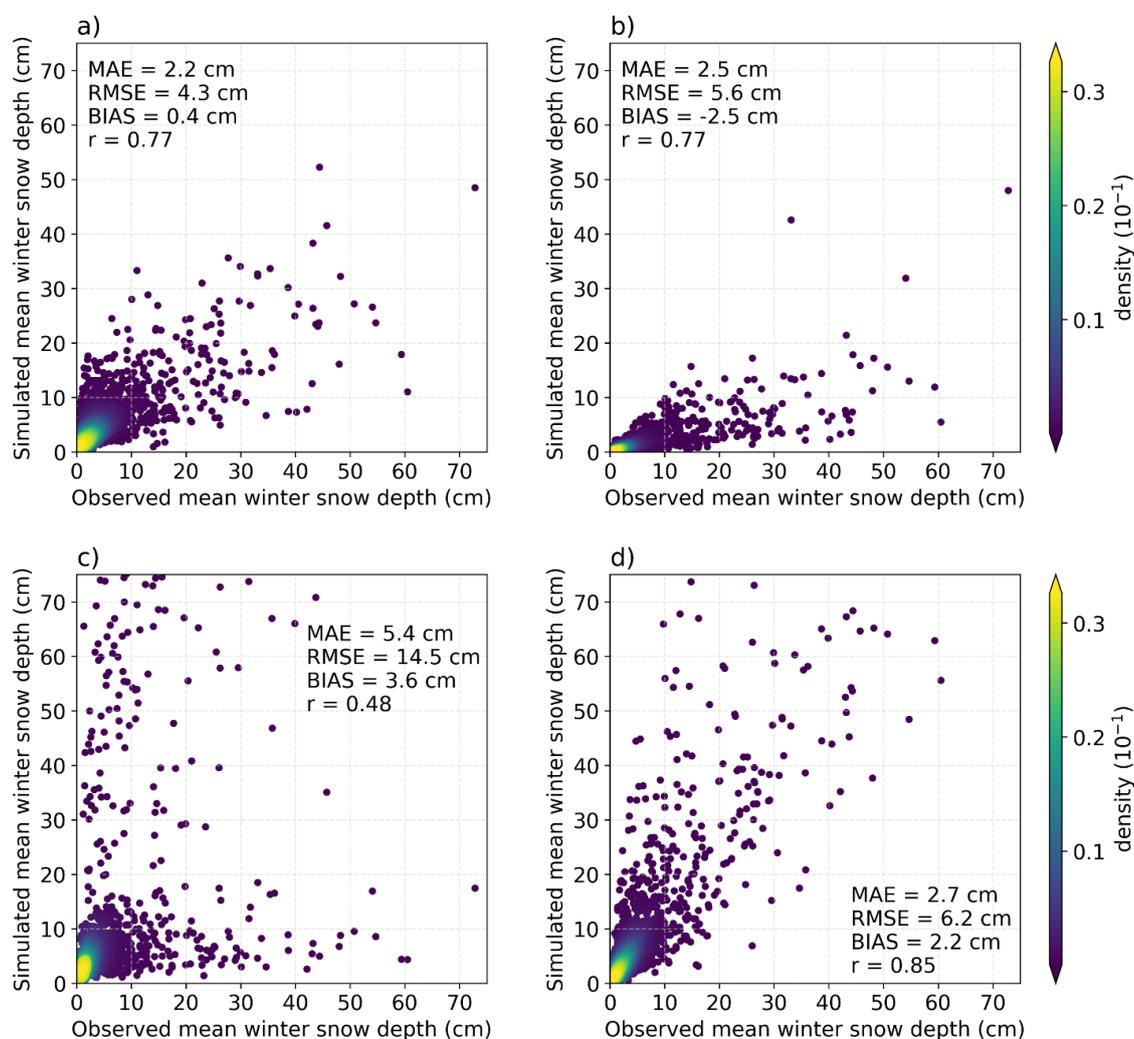

Figure 7: Mean winter snow depth for each winter season and location in 1987 – 2018 simulated by the WRF model (a), CCLM (b),
290 **ERA5L (c), and AMUNDSEN (d).**

The Cryosphere
Discussions

Open Access

EGU

3.3 Snow cover duration

Mapping the snow cover duration averaged for 1987 – 2018 shows similar spatial patterns as the mean snow depth (compare Fig. 8 to Fig. 6), which also applies for the differences to the observations. CCLM generally underestimates the duration (Fig. 8b), whereas ERA5L generally overestimates apart from four locations in the northern middle mountain ranges (Fig. 8c). WRF and AMUNDSEN show lower differences with a similar spatial pattern (Fig. 8a and 8d).

The separate evaluation of each year is presented in Figure 9, where the low bias of less than 7 days is confirmed for WRF and AMUNDSEN. CCLM predicts on average 20 days less snow cover than observed. However, the rank correlation of each year and station is well reproduced (r = 0.85). ERA5L on the opposite simulates the duration on average 34 days too long.
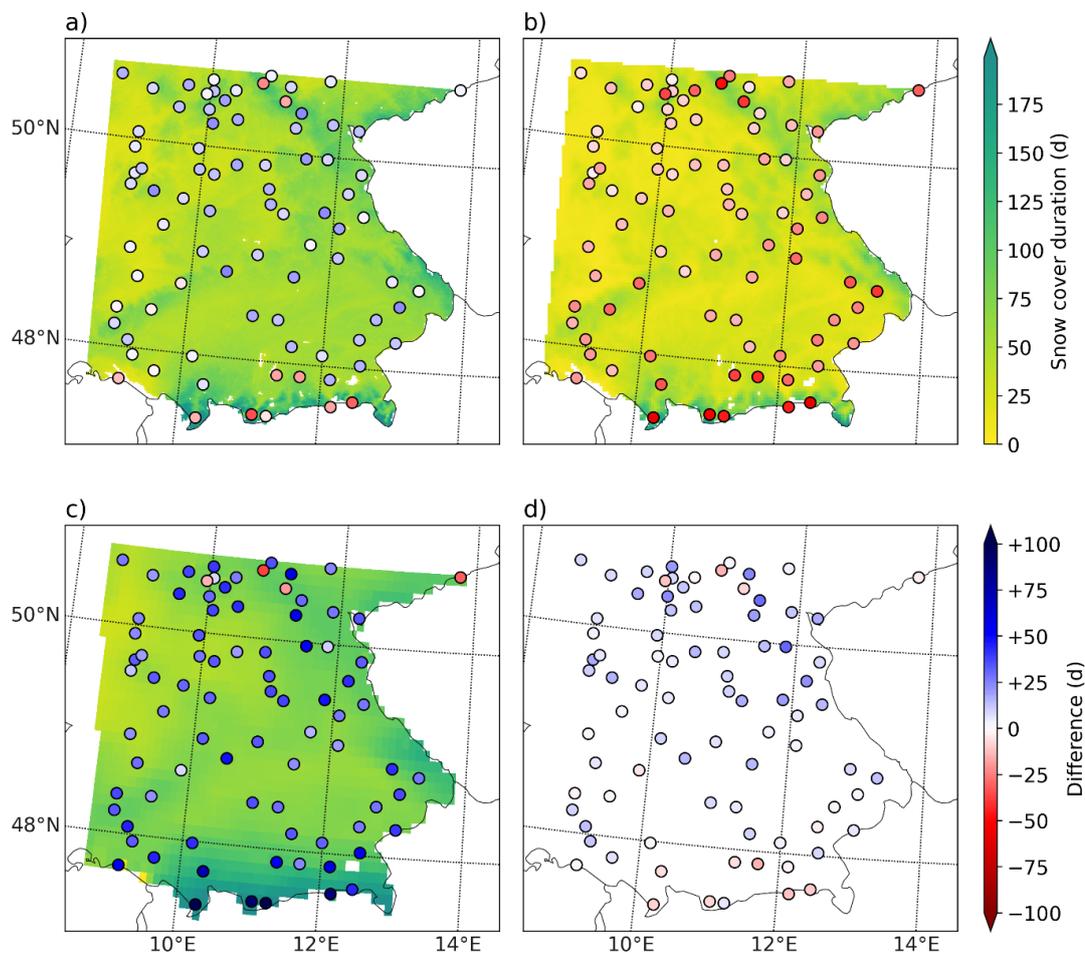
Figure 8: Mean annual snow cover duration during 1987 – 2018 simulated by the WRF model (a), CCLM (b), ERA5L (c), and AMUNDSEN (d). Snow cover duration is defined as the number of days with more than 0.01 m snow depth. The differences at the stations (coloured dots) are calculated as model minus observation. Red (blue) colour refers to an under- (over)estimation of the model.
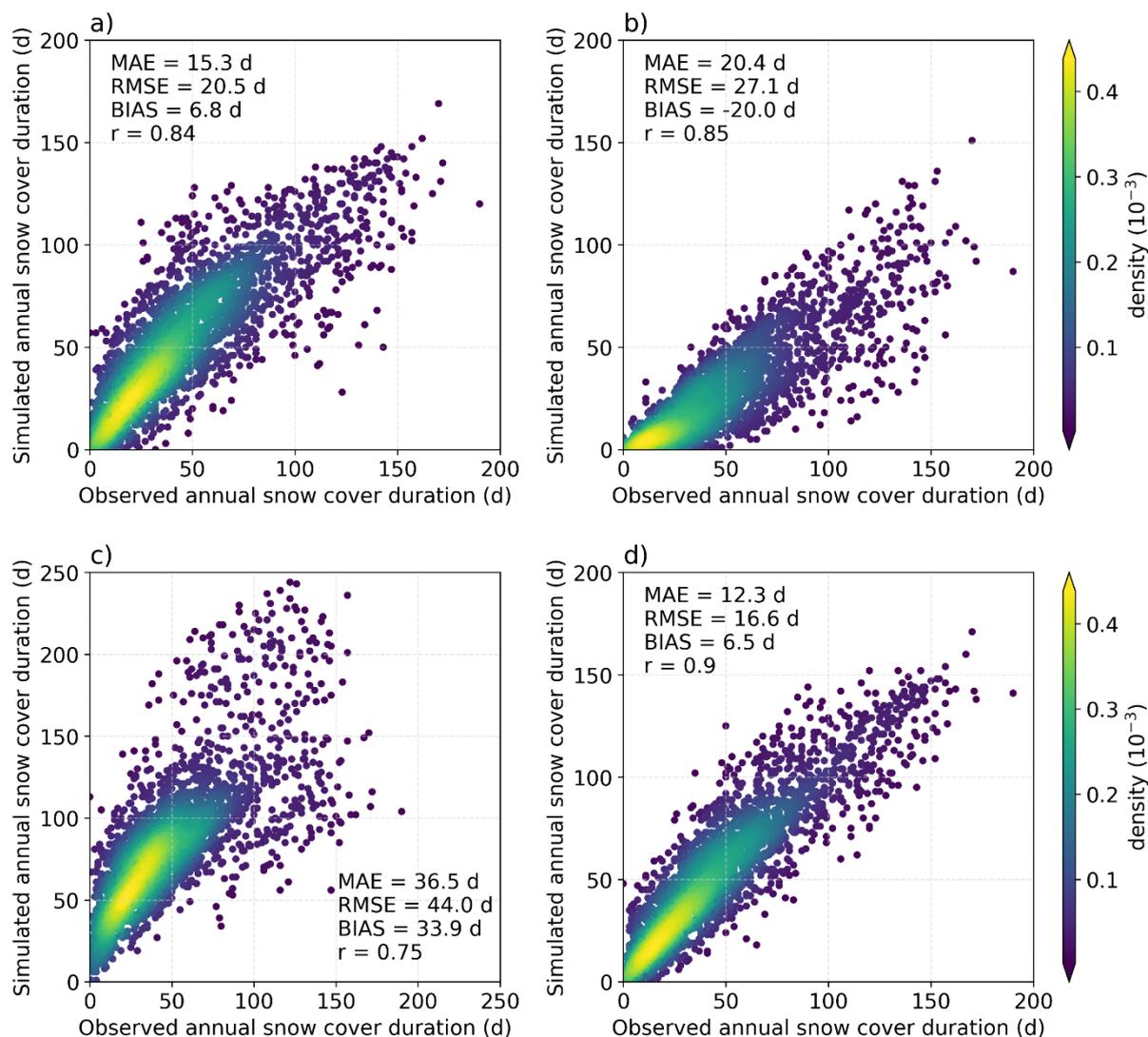
Figure 9: Annual snow cover duration for each year and location in 1987 – 2018 simulated by the WRF model (a), CCLM (b), ERA5L (c), and AMUNDSEN (d).

3.4 White Christmas

These mean seasonal deviations also manifest when assessing smaller time periods than seasonal averages. The percentage of white Christmas during 1987 – 2018 results in four very different predictions (Fig. 10). The spatial pattern follows the previous evaluations of mean snow depth and snow cover duration (compare Fig. 10 to Fig. 6 and 8). Averages over all seasons and locations are provided in Table 3. There, the CCLM and AMUNDSEN outperform WRF and ERA5L, but the percentages of

The Cryosphere
Discussions

315 false positives and false negatives of white Christmas are still substantial compared to the observed percentage of 22.9 % white

Christmas.
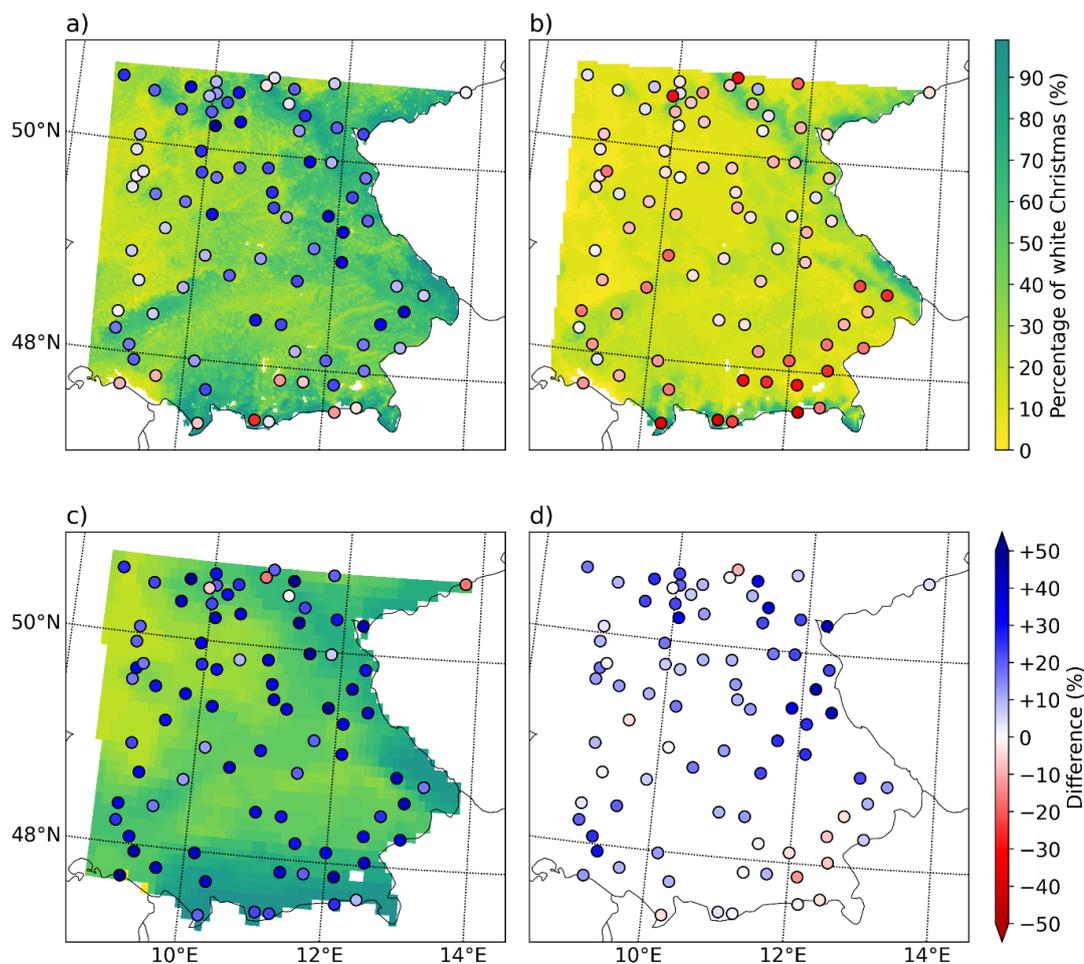
Figure 10: Percentage of white Christmas during 1987 – 2018 simulated by the WRF model (a), CCLM (b), ERA5L (c), and AMUNDSEN (d). White Christmas is defined as more than 0.01 m snow depth on either the 24th, 25th, or 26th of December. The
320 **differences at the stations (coloured dots) are calculated as model minus observation. Red (blue) colour refers to an under-(over)estimation of the model.**

325

330   **Table 3: Percentages of white Christmas averaged over all 1987 – 2018 and all locations in the study area.**

	WRF	CCLM	ERA5L	AMUNDSEN
Correct prediction	76.3 %	89.0 %	69.3 %	84.7 %
…thereof white Christmas	19.8 %	14.1 %	22.4 %	20.9 %
…thereof non-white Christmas	56.5 %	74.9 %	46.9 %	63.8 %
False positives	20.6 %	2.2 %	30.2 %	13.3 %
False negatives	3.1 %	8.8 %	0.5 %	2.0 %

4 Evaluation of extreme snow dynamics

Extremes of snow dynamics are causing different environmental risks. Here, we investigate extreme snow depths, extreme daily snow accumulations, and extreme daily snow melting.

335   ### 4.1 Annual maximum daily snow depth

Figure 11 provides the simulated and observed maxima of snow depth, where the WRF model shows the smallest errors and almost no bias. Observed high snow depths are slightly underestimated (Fig. 11a). The general underestimation of CCLM also applies for the maximum snow depths (Fig. 11b). The percentage bias of -60.3 % suggests that the model is not appropriate to assess extreme snow depths, as already described in the documentation by Doms et al. (2021). The rank correlation of $r = 0.84$

340   however suggests, that the model is able to well reproduce inter-site and interannual differences. ERA5L tends to overestimate extreme snow depths on average yielding the highest RMSE and lowest rank correlation. The largest deviations occur for snow depths above 0.5 m in complex topography. The difference of the mean annual maximum snow depth for the 83 stations correlates strongly with the elevation bias of ERA5L (see Fig. 4c and Tab. S3; $r = 0.91$) indicating that the spatial resolution is too low to analyse extreme snow dynamics in the middle mountain ranges and Alps. For the other models, no significant

345   correlation is found for this dependence. AMUNDSEN slightly overpredicts extreme snow depths with a moderate positive bias of 15.1 %.

We assess, if the GEV location parameters µ fitted on the modelled annual maxima of snow depth are within the 95 % confidence interval of the respective observation-based µ for each station (see Figure S4). We find that the CCLM is not able to reproduce this extreme value statistical property within the observational range at any station. AMUNDSEN shows the

350   highest agreement with 57% of stations, followed by WRF (51%) and ERA5L (34%). ERA5L cannot capture the rank correlation between the stations ($r = 0.61$) as well as the other models ($r > 0.91$). The WRF model shows good agreement for stations with location parameters below 20 mm but underestimates the upper range (Fig. S4).

The seasonality of the annual maximum snow depth is visualized as bivariate kernel density estimation (Figure 12). The general timing of annual maximum snow depths is reproduced well by all models (compare the marginal histograms in Fig. 12), whereby the CCLM simulates not enough snow depth maxima after February (Fig. 12b). For the comparison of each station-year combination in 1987 – 2018, the WRF model (Fig. 12a) shows the highest agreement with low bias.
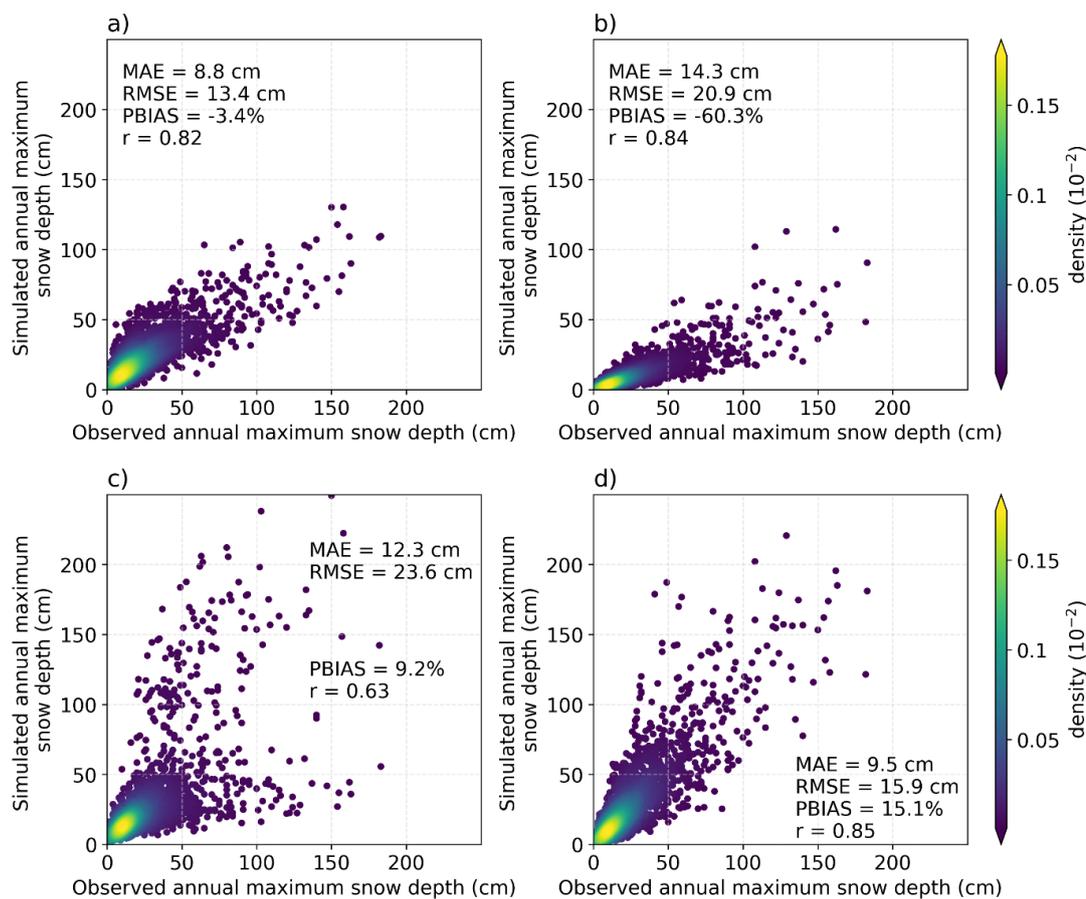

Figure 11: Annual maxima of snow depth for each year and location in 1987 – 2018 simulated by the WRF model (a), CCLM (b), ERA5L (c), and AMUNDSEN (d).
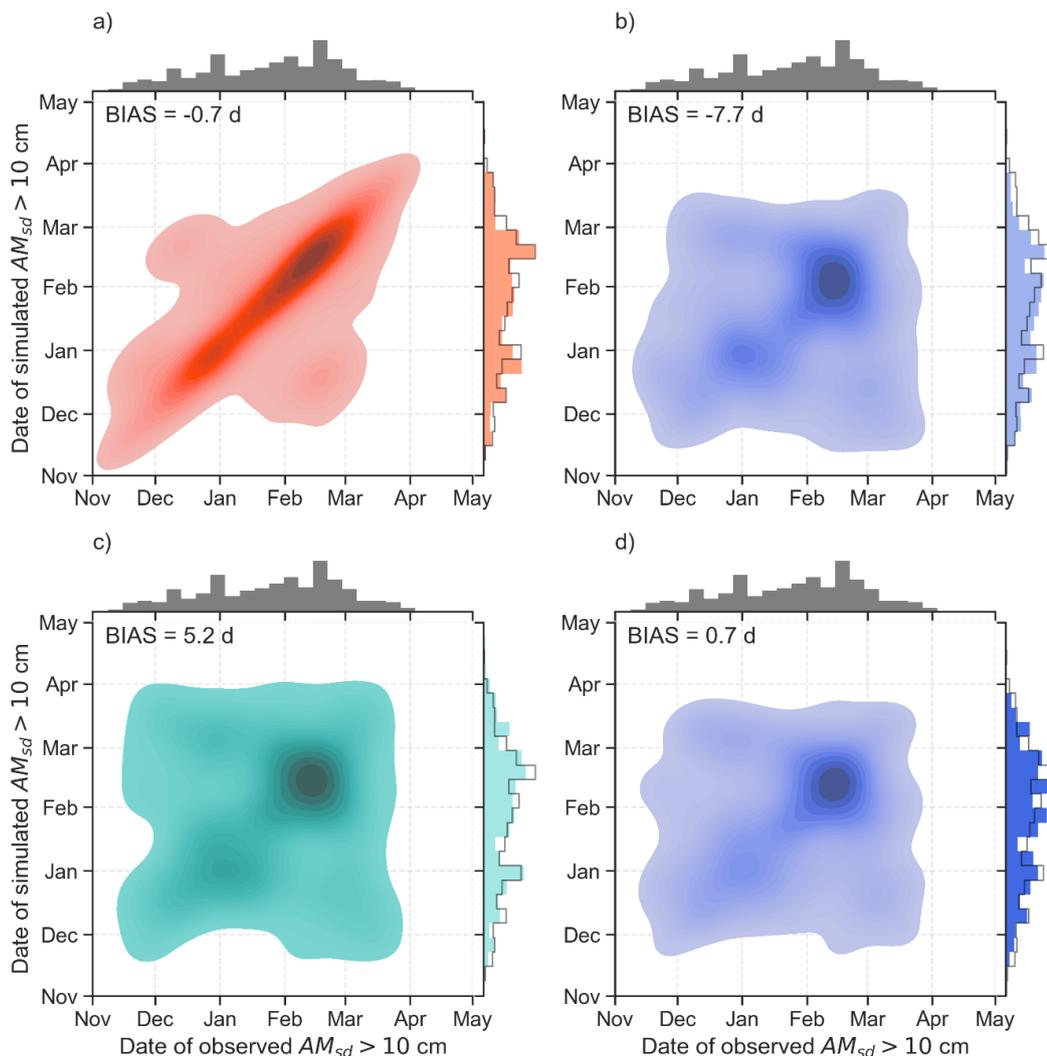
Figure 12: Bivariate kernel density plot of dates for annual maxima snow depth above 10 cm for each year and location in 1987 – 2018 simulated by the WRF model (a), CCLM (b), ERA5L (c), and AMUNDSEN (d). The marginal distributions aggregated over all years and stations are given as histogram aside, where the grey histogram and grey line histogram refer to the observations.
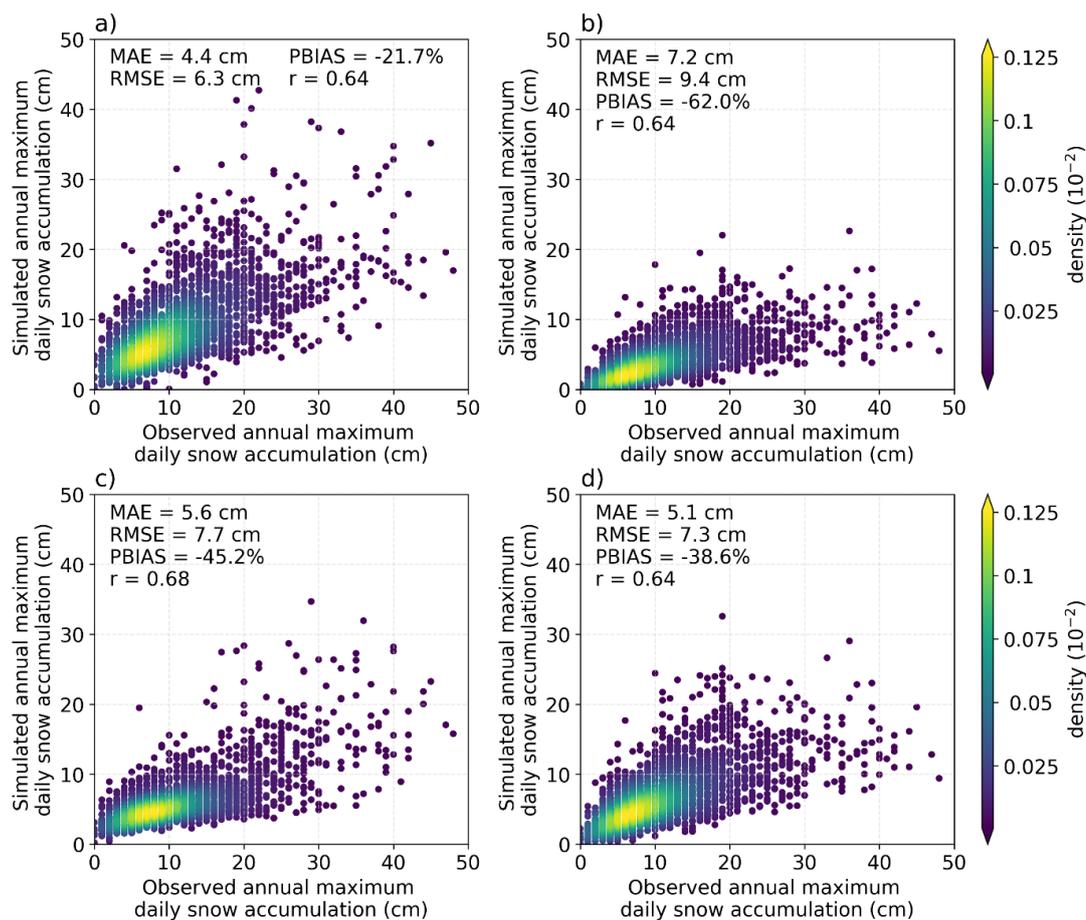
365

4.2 Annual maximum daily snow accumulation

The observed and modelled daily maximum snow accumulation for each year and station is provided in Figure 13. All models show a negative bias and similar rank correlation. The general underestimation of daily snow accumulation extremes within WRF, CCLM, and ERA5L may be partly caused by comparing areal simulations to point observations. Extreme daily snowfall

370 is highly variable in space and time and an areal average smooths the variability and therefore lowers the resulting extreme

20

values. The lowest errors are diagnosed for the WRF simulations. The CCLM only predicts two days with slightly more than 0.2 m snow accumulation, whereas the observations cover the range from 0 to 0.5 m. The corresponding seasonality is provided in Figure S5.
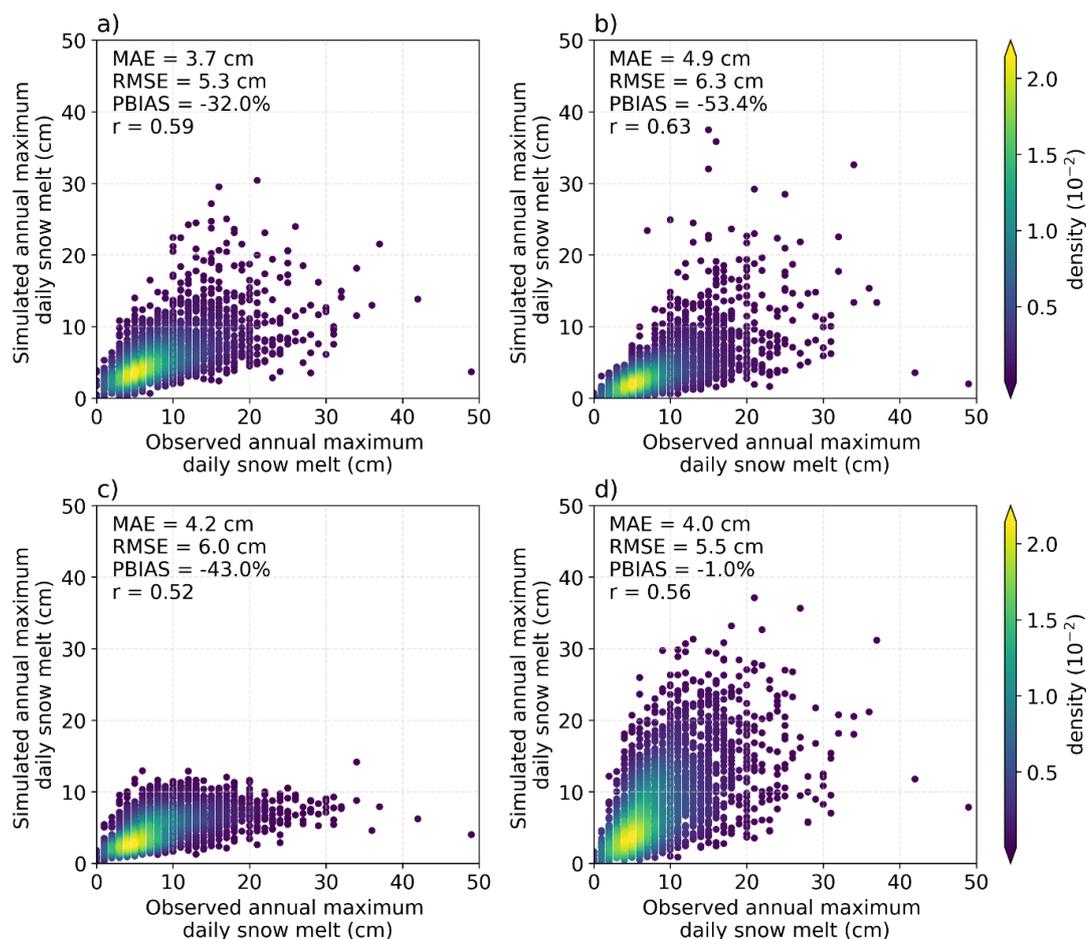

Figure 13: Annual maxima of daily snow depth accumulation for each year and location in 1987 – 2018 simulated by the WRF model (a), CCLM (b), ERA5L (c), and AMUNDSEN (d).

4.3 Annual maximum daily snow melt

WRF, CCLM, and ERA5L show a negative bias meaning too low snow melt volumes (Fig. 14), which may be partly caused by the comparison of areal simulations to point observations. Only AMUNDSEN can reproduce the extreme melting without bias. The maxima of snow melt from the ERA5L simulations reach 0.15 m at the most, whereas the observations cover 0 to 0.5 m. Since ERA5 overestimates the absolute snow depth (Fig. 7c) and its extremes (Fig. 11c), there would be enough simulated snow depths to reach extreme melting heights. For the CCLM, the negative bias of daily snow melt extremes can be partly attributed to the fact that the absolute extremes of snow depths are underestimated, restricting extreme snow melt when

385   all snow has already melted. This can be seen, for example, in Figure 5 for the 2005/2006 season in March, where a strong

snow melt was measured. In the CCLM simulation, in contrast to the other models, the preceding snow depth was so low that

no large melt height could be reached. The observed and simulated seasonality are shown in Figure S6.

Figure 14: Annual maxima of daily snow melt for each year and location in 1987 – 2018 simulated by the WRF model (a), CCLM
390   **(b), ERA5L (c), and AMUNDSEN (d).**


5 Discussion of uncertainties

The representation of snow dynamics is important for impact assessments (see Section 1) and for the coupling within the

regional climate model in case of the WRF and CCLM.

395   Depending on the measure of interest, the evaluation yields very different results, even though all simulations are driven by

the same large-scale atmospheric conditions from ERA5. This indicates the large model uncertainties regarding snow

dynamics. These uncertainties result from different sources and are interconnected, which is why they are difficult to disentangle.

In Table 2, the significant correlation between elevation bias and the biases of temperature and precipitation for ERA5L can
400 be referred to the spatial resolution of the model. Due to the 9 km grid cell size, the complexity of the terrain cannot be reproduced in parts of the study area. For the WRF simulation, a significant correlation between elevation and temperature bias is found indicating that the lower elevated stations show a more pronounced cold bias. Overall, the WRF shows a systematic underestimation of temperature. Collier and Mölg (2020) refer this behaviour to a miscalculation of the mean grid cell albedo in the NOAH_MP (Tomasi et al., 2017). Generally, it should be emphasized that the albedo of exposed snow
405 surfaces differs from snow over surfaces with shrub or forest vegetation. The areal simulations of WRF, CCLM, and ERA5L represent mean grid cell values and depend on the land cover parametrization of the respective grid cell. At the point of the climate station, exposed snow areas predominate due to the standardised environmental conditions with grass cover. Hence, the comparability is limited for grid cells, where the model assumes forest. Furthermore, the temporal variability of snow and albedo at the point scale can be higher than for areal averages (Clark et al., 2011). Remote sensing products provide
410 observation-based areal estimations for the albedo. We compare the albedo of the WRF, CCLM, and ERA5L simulations to the remote sensing product MODIS MCD43C3 at 0.05° resolution (Schaaf and Wang, 2021) for the whole study area without the Alps (Fig. 15a) and the Alps only (Fig. 15b) and confirm the strong overestimation within the WRF simulation. ERA5L agrees over the non-alpine area, however overestimating in the Alps, where the strongest deviations occur during early and late winter reflecting the huge positive bias in the snow cover duration in the Alps (Fig. 8c). As ERA5L is an offline simulation
415 driven by the climate of ERA5, the simulated albedo of ERA5L has only very minor effects on the temperatures shown in Figure 3. The empirical parametrization in CCLM agrees with MODIS during the first months (until mid-January and beginning of February, respectively), however underestimates the albedo afterwards. This is due to the underestimation of snow cover duration (Figs. 9b & 10b). As the land surface scheme TERRA_ML is run coupled with the atmospheric simulation, the albedo affects the simulated air temperature. However, the low biases in temperature (Fig. 3) suggest that the overall
420 representation of the albedo in TERRA_ML does not translate to strong discrepancies in temperature of CCLM.

23
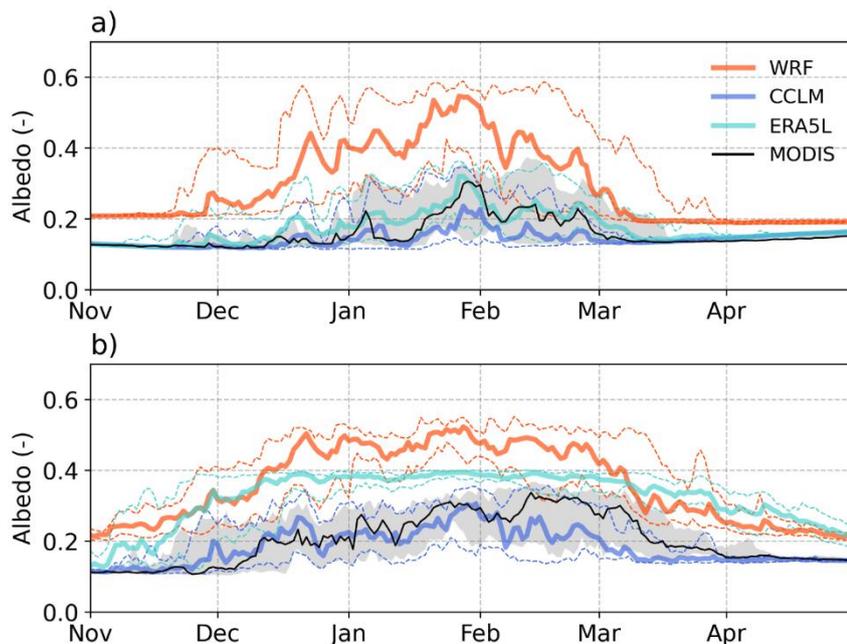
Figure 15: Albedo for the years 2000 to 2018. Daily albedo values are averaged over the whole study area (a) without the Alps and
(b) for the Alps (south of 47.8 °N and west of 10° E) only. The thick lines denote the median over all seasons. The area between the
dashed lines and the grey transparent area show the inner 50% range. For the remote sensing product (MODIS MCD43C3), only
data with at least "mixed" or good quality are considered, where at least half of the area needs to be covered with valid values.

The different albedo simulations are compared over one selected winter season and five locations (Fig. S7, Tab. S8). There,
the negative temperature bias of the WRF simulations (Fig. 3) occurs mainly during periods with snow and therefore
overestimated snow albedo (Fig. S9) confirming the assumption by Collier and Mölg (2020). Liu et al. (2021) propose a
modified snow albedo scheme for the NOAH_MP with on average lower albedo values than the default scheme improving the
representation of sensible heat flux, air temperature, and snow depth over the Tibetan Plateau. The albedo scheme of
AMUNDSEN for exposed snow surfaces yields a similar albedo estimation as the WRF simulation for non-forested grid cells
(Fig. S7). However, AMUNDSEN represents the point scale and is not run coupled with the atmospheric modelling therefore
not affecting the modelled climate.

Furthermore, the snow surface albedo also governs the energy budget of the snow layer (Essery et al., 2013). The slight
overestimation in mean snow depth and snow cover duration of the WRF simulations can be attributed to the biases in albedo
and temperature. Applying different albedo parametrizations induces considerable differences in the simulated snow depth and
snow cover duration. For the WRF simulations, 17 of the 83 locations are classified as forest. The mean bias of winter snow
depth and snow cover duration amount to +0.4 cm and +6.8 d (Figs. 7a and 9a). For the 17 forest grid cells, however, the
deviations amount to -0.9 cm and +3.2 d, whereas the remaining non-forested locations show larger overestimations of snow
dynamics (+0.9 cm and +7.7 d).

24

Even though ERA5L simulates a lower surface albedo over non-forested areas than WRF, it shows the strongest positive bias

445 in mean snow depth and snow cover duration. The largest overestimations are located in the (pre-)alpine areas in the south of the study area, however, the snow cover duration is overestimated for almost the whole region. Daloz et al. (2022) also report positive deviations of ERA5L in the extent, fraction, and duration of snow cover over Europe compared to MODIS. Kouki et al. (2023) find in an evaluation with various satellite-based data that ERA5L also overestimates the snow water equivalent in the Northern Hemisphere in spring. When developing the new snow scheme for the next generation ECLand model (Bousetta

450 et al., 2021), these deviations should be accounted for.

Despite the skilful reproduction of precipitation and air temperature (Fig. 3b and 3e) and realistic ranges of simulated albedo (Figs. 15 & S7), the CCLM simulates snow depth and snow cover duration with large negative biases suggesting that the snow scheme is not appropriate for any further impact analysis.

Based on the same climatic conditions, AMUNDSEN tends to slightly overpredict snow depth and snow cover duration. The

455 larger overestimations of the AMUNDSEN simulation are located in the middle mountain ranges (Fig. 6d and 8d). Especially during snowy winter seasons, AMUNDSEN produces snow depths that are heavily overestimated. An exploration of these locations reveals that the CCLM has a general positive precipitation bias there, which is partly diagnosed by the rank correlation of $r = 0.32$ between elevation and precipitation bias. However, this positive bias mostly applies for the stations above 500 m elevation north of 48.5° N (Fig. S10).

460 Apart from the sources of uncertainties discussed above, also the parametrization of snow density adds uncertainty (Essery et al., 2013). Here, the models all follow different flavours of the parametrization of density and compaction by Anderson et al. (1976). At the climate stations, snow density or snow water equivalent is not measured and can therefore not be evaluated. In addition, the number of considered snow layers is found relevant for the reproduction of snow depth and cover (Arduini et al., 2019; Jin et al., 1999). Jin et al. (1999) emphasize that multiple snow layers improve the representation of temporal variability

465 within diurnal and seasonal time scales. Xue et al. (2003) highlight the importance of multiple snow layers for the ablation period, as multiple layers are able to separate soil temperature and surface temperature. This is considered beneficial for reproducing the variability of snow surface temperatures, while single-layer setups tend to simulate surface temperatures around the freezing point with little variability. Here, the multi-layer setups of WRF and AMUNDSEN show a better performance of the snow cover duration, timing and intensity of annual maximum daily snow melt. The new five-layer snow

470 scheme of ECLand (Arduini et al., 2019) improves the simulation of melting periods compared to the single-layer scheme of ERA5L, however the performance of daily extremes melting was not investigated.

The evaluation of simulations for limited periods of the year would be very relevant for tourism related topics. Here, the ability to predict white Christmas is assessed, with all simulations showing large deviations from the observations. This means that many tourism-oriented studies with predefined holiday periods cannot be carried out meaningfully due to these uncertainties.

475 For the representation of extremes in snow depth, daily accumulation and melting rates, the differences between the point scale and areal simulations may affect the comparison. Averaged over all locations, one would expect a slight underestimation of simulated annual maximum snow depth as the climate station shows an exposed snow surface, whereas grid cells may represent

mixed surfaces or forested areas. For daily accumulation and melting rates, the point scale shows a higher temporal variability than areal averages therefore leading to more pronounced extremes. Still considering these limitations, the assessment reveals

480   that WRF and AMUNDSEN can clearly add value to the representation of extremes compared to ERA5L.

6 Conclusions and recommendations

In conclusion, the high-resolution climate model WRF and the hydro-climatological model AMUNDSEN driven by CCLM can add value compared to the state-of-the-art reanalysis product ERA5L. The CCLM shows a skilful reproduction of the climate but systematically underestimates all snow dynamics. Based on this assessment, one can draw some recommendations

485   for model application and further model development.

First, simulations of snow dynamics have to be carefully evaluated according to the further intended use of the data. This evaluation has shown that the setup of the regional climate model or land surface model can largely influence the snow depth simulations, even if they are all driven by the same large-scale atmospheric conditions. With coarse-resolution climate models, the complexity of the terrain often prevents comparability between the results of the climate model and the observations. For

490   the 83 locations in southern Germany with a terrain with different degrees of complexity, the resolution of the high-resolution RCMs is sufficient to reproduce the elevations with moderate to low deviations. For the representation of the winter climate, high-resolution RCMs can add value compared to ERA5L. This translates also to a benefit for the representation of snow dynamics, except if the snow model is not appropriately parametrized for the study area (as in the case of CCLM and TERRA_ML). In case of a well-represented climate but strong biases in the snow simulation, the added value of the high-

495   resolution climate simulation can be utilized by setting up a separate snow model calibrated to the local conditions. Hence, for local and regional snow impact assessments, high-resolution climate models can be a valuable tool. However, we recommend to analyse climate and snow biases carefully.

Second, for future climate model and land surface model development, the evaluation in this study has revealed some potential for improvement. A revision of the TERRA_ML snow scheme in the ICON-CLM model is recommended. For the NOAH_MP,

500   the problem of too high albedos has been addressed by Tomasi et al. (2017) and the resulting cold bias during winter as well as overestimation of snow dynamics are confirmed for southern Germany in this study. New albedo parametrizations are already proposed (Liu et al., 2021). The overprediction of mean snow depth and snow cover duration in the ERA5L simulations partly result from the elevation bias and according temperature bias. However, the general tendency to overestimate snow cover duration and the underestimation of extreme daily snow melting indicate that the snow scheme needs to be revised

505   accordingly in the course of the development of the new ECLand model.

Generally, parametrizations and snow models tend to be developed and evaluated disproportionately in alpine and arctic areas (e.g. Essery et al., 2013, Krinner et al., 2018, Liu et al., 2021). This is understandable as snow dynamics have high relevance there and long records without non-natural influences are available. However, considering the relevance for snow-related impacts, it is also important that snow dynamics in more densely populated areas are well represented in the simulations.

510 Hence, we propose the study area in southern Germany as testbed for further investigations such as the LUCAS phase 3 (Daloz et al., 2022).

On the other hand, high-resolution climate model or earth system model simulations could further improve our knowledge of snow dynamics in topographically highly complex regions, where state-of-the-art reanalysis data and earth system models show large deviations from observations (Daloz et al., 2020; Kouki et al., 2022). However, observations are sparsely distributed

515 in these regions. Snowfall and snow storage play an important role in freshwater availability, with strong implications of rising temperatures (Simpkins, 2018). Hence, high-resolution models could support decision-making regarding water infrastructure design and management.

Lastly, we recommend to evaluate the performance of snow models regarding extreme snow dynamics. Possible measures are proposed in this study, such as daily maxima of snow depth, accumulation, melting and their seasonality. Our knowledge about

520 future snow dynamics depends on model simulations. Due to the high impacts of extreme snow conditions on the human society, it is relevant to capture these events in the simulations.

References

Anderson, E. A.: A point energy and mass balance model of a snow cover, Tech. Rep. NWQ 19, NOAA, Office of Hydrology, National Weather Service, Silver Spring, MD, USA, available at: https://repository.library.noaa.gov/view/noaa/6392 (last access: 19 July 2023), 1976.

Arduini, G., Balsamo, G., Dutra, E., Day, J. J., Sandu, I., Boussetta, S., and Haiden, T.: Impact of a Multi-Layer Snow Scheme on Near-Surface Weather Forecasts, J. Adv. Model. Earth Sy., 11, 4687–4710, https://doi.org/10.1029/2019MS001725, 2019.

Barnett, T. P., Adam, J. C., and Lettenmaier, D. P.: Potential impacts of a warming climate on water availability in snow-dominated regions, Nature, 438, 303–309, https://doi.org/10.1038/nature04141, 2005.

Bausch, T. and Unseld, C.: Winter tourism in Germany is much more than skiing! consumer motives and implications to Alpine destination marketing, J. Vacat. Mark., 24, 203–217, https://doi.org/10.1177/1356766717691806, 2018.

Bednorz, E.: Heavy snow in Polish–German lowlands: large-scale synoptic reasons and economic impacts, Weather and Climate Extremes, 2, 1–6, https://doi.org/10.1016/j.wace.2013.10.007, 2013.

Berghuijs, W. R., Harrigan, S., Molnar, P., Slater, L. J., and Kirchner, J. W.: The relative importance of different flood-generating mechanisms across Europe, Water Resour. Res., 55, 4582–4593, https://doi.org/10.1029/2019WR024841, 2019.

Blume-Werry, G., Kreyling, J., Laudon, H., and Milbau, A.: Short-term climate change manipulation effects do not scale up to long-term legacies: effects of an absent snow cover on boreal forest plants, J. Ecol., 104, 1638–1648, https://doi.org/10.1111/1365-2745.12636, 2016.

Bocharov, G.: pyextremes - Extreme Value Analysis (EVA) in Python, available at: https://georgebv.github.io/pyextremes/ (last access: 19 July 2023), 2022.

Boussetta, S., Balsamo, G., Arduini, G., Dutra, E., McNorton, J., Choulga, M., Agustí-Panareda, A., Beljaars, A., Wedi, N., Muñoz Sabater, J., de Rosnay, P., Sandu, I., Hadade, I., Carver, G., Mazzetti, C., Prudhomme, C., Yamazaki, D., and Zsoter, E.: ECLand: The ECMWF Land Surface Modelling System, Atmosphere, 12, 723, https://doi.org/10.3390/atmos12060723, 2021.

Braun, L. N.: Simulation of snowmelt-runoff in lowland and lower alpine regions of Switzerland, Ph.D. thesis, ETH Zurich, 1984.

Brienen, S., Haller, M., Brauch, J., and Früh, B.: HoKliSim-De COSMO-CLM climate model simulation data version V2022.01 [data set], https://dx.doi.org/10.5676/DWD/HOKLISIM_V2022.01, 2022.

Chen, J., Li, C., Brissette, F. P., Chen, H., Wang, M., and Essou, G. R. C.: Impacts of correcting the inter-variable correlation of climate model outputs on hydrological modeling, J. Hydrol., 560, 326–341, https://doi.org/10.1016/j.jhydrol.2018.03.040, 2018.

Clark, M. P., Hendrikx, J., Slater, A. G., Kavetski, D., Anderson, B., Cullen, N. J., Kerr, T., Hreinsson, E. O., and Woods, R. A.: Representing spatial variability of snow water equivalent in hydrologic and land-surface models: A review, Water Resour. Res., 47, W07539, https://doi.org/10.1029/2011wr010745, 2011.

575   Coles, S.: An introduction to statistical modeling of extreme values, Springer, London, UK, 2001.

Collier, E.: BAYWRF, OSFHOME [data set], https://doi.org/10.17605/OSF.IO/AQ58B, 2020.

Collier, E. and Mölg, T.: BAYWRF: a high-resolution present-day climatological atmospheric dataset for Bavaria, Earth Syst. Sci. Data, 12, 3097–3112, https://doi.org/10.5194/essd-12-3097-2020, 2020.

Coppola, E., Sobolowski, S., Pichelli, E., Raffaele, F., Ahrens, B., Anders, I., Ban, N., Bastin, S., Belda, M., Belusic, D.,
580   Caldas-Alvarez, A., Cardoso, R. M., Davolio, S., Dobler, A., Fernandez, J., Fita, L., Fumiere, Q., Giorgi, F., Goergen, K., Güttler, I., Halenka, T., Heinzeller, D., Hodnebrog, Q., Jacob, D., Kartsios, S., Katragkou, E., Kendon, E., Khodayar, S., Kunstmann, H., Knist, S., Lavín-Gullón, A., Lind, P., Lorenz, T., Maraun, D., Marelle, L., van Meijgaard, E., Milovac, J., Myhre, G., Panitz, H. J., Piazza, M., Raffa, M., Raub, T., Rockel, B., Schär, C., Sieck, K., Soares, P. M. M., Somot, S., Srnec, L., Stocchi, P., Tölle, M. H., Truhetz, H., Vautard, R., de Vries, H., and Warrach-Sagi, K.: A first-of-its-kind multi-model
585   convection permitting ensemble for investigating convective phenomena over Europe and the Mediterranean, Clim. Dynam., 43, 3–34, https://doi.org/10.1007/s00382-018-4521-8, 2020.

Croce, P., Formichi, P., Landi, F., Mercogliano, P., Bucchignani, E., Dosio, A., and Dimova, S.: The snow load in Europe and the climate change, Climate Risk Management, 20, 138–154, https://doi.org/10.1016/j.crm.2018.03.001, 2018.

Daloz, A. S., Mateling, M., L'Ecuyer, T., Kulie, M., Wood, N. B., Durand, M., Wrzesien, M., Stjern, C. W., and Dimri, A. P.:
590   How much snow falls in the world's mountains? A first look at mountain snowfall estimates in A-train observations and reanalyses, The Cryosphere, 14, 3195–3207, https://doi.org/10.5194/tc-14-3195-2020, 2020.

Daloz, A. S., Schwingshackl, C., Mooney, P., Strada, S., Rechid, D., Davin, E. L., Katragkou, E., de Noblet-Ducoudré, N., Belda, M., Halenka, T., Breil, M., Cardoso, R. M., Hoffmann, P., Lima, D. C. A., Meier, R., Soares, P. M. M., Sofiadis, G., Strandberg, G., Toelle, M. H., and Lund, M. T.: Land-atmosphere interactions in sub-polar and alpine climates in the CORDEX
595   FPS LUCAS models: I. Evaluation of the snow-albedo effect, The Cryosphere, 16, 2403–2419, https://doi.org/10.5194/tc-16-2403-2022, 2022.

Doll, C., Trinks, C., Sedlacek, N., Pelikan, V., Comes, T., and Schultmann, F.: Adapting rail and road networks to weather extremes: case studies for southern Germany and Austria, Nat. Hazards, 72, 63–85, https://doi.org/10.1007/s11069-013-0969-3, 2014.

600   Doms, G., Förstner, J., Heise, E., Herzog, H. J., Mironov, D., Raschendorfer, M., Reinhardt, T., Ritter, B., Schrodin, R., Schulz, J.-P., and Vofel, G.: A Description of the Nonhydrostatic Regional COSMO-Model – Part II: Physical Parameterizations, Deutscher Wetterdienst DWD, Offenbach, 2021.

Durre, I. and Squires, M. F.: White Christmas? An Application of NOAA's 1981–2010 Daily Normals. Bull. Am. Meteorol. Soc., 96, 1853-1858, https://doi.org/10.1175/BAMS-D-15-00038.1, 2015.

605   Dutra, E., Balsamo, G., Viterbo, P., Miranda, P. M., Beljaars, A., Schär, C., and Elder, K.: An improved snow scheme for the ECMWF land surface model: description and offline validation, J. Hydrometeorol., 11, 899–916, https://doi.org/10.1175/2010JHM1249.1, 2010.

DWD (German Weather Service): Weiße Weihnachten – eine Frage des Standortes, available at: https://www.dwd.de/DE/wetter/thema_des_tages/2020/12/24.html (last access: 19 July 2023), 2020.

610   DWD (German Weather Service): Daily climate data [data set], https://opendata.dwd.de/climate_environment/CDC/observations_germany/climate/daily/kl/historical/, 2023.

ECMWF (ed.): IFS documentation Cy45r1 Operational implementation 5 June 2018 PART IV: physical processes. pp. 223, Shinfield Park, Reading, England, UK available at: https://www.ecmwf.int/en/elibrary/80895-ifs-documentation-cy45r1-part-iv-physical-processes (last access: 19 July 2023), 2018.

615   Essery, R., Morin, S., Lejeune, Y., and Ménard, C.: A comparison of 1701 snow models using observations from an alpine site, Adv. Water Res., 55, 131–148, https://doi.org/10.1016/j.advwatres.2012.07.013, 2013.

Foreman-Mackey, D., Hogg, D. W., Lang, D., and Goodman, J.: emcee : The MCMC Hammer, Publ. Astron. Soc. Pacific, 125(925), 306–312, https://doi.org/10.1086/670067, 2013.

Frei, P., Kotlarski, S., Liniger, M. A., and Schär, C.: Future snowfall in the Alps: projections based on the EURO-CORDEX
620   regional climate models, The Cryosphere, 12, 1–24, https://doi.org/10.5194/tc-12-1-2018, 2018.

Gavazov, K., Ingrisch, J., Hasibeder, R., Mills, R. T. E., Buttler, A., Gleixner, G., Pumpanen, J., and Bahn, M.: Winter ecology of a subalpine grassland: effects of snow removal on soil respiration, microbial structure and function, Sci. Tot. Environ., 590–591, 316–24, https://doi.org/10.1016/j.scitotenv.2017.03.010, 2017.

Gerhold, L., Wahl, S., and Dombrowsky, W. R.: Risk perception and emergency food preparedness in Germany, Int. J. Disaster
625   Risk Reduct., 37, 101183, https://doi.org/10.1016/j.ijdrr.2019.101183, 2019.

Girons Lopez, M., Vis, M. J. P., Jenicek, M., Griessinger, N., and Seibert, J.: Assessing the degree of detail of temperature-based snow routines for runoff modelling in mountainous areas in central Europe, Hydrol. Earth Syst. Sci., 24, 4441–4461, https://doi.org/10.5194/hess-24-4441-2020, 2020.

Hammer, H. L.: Statistical models for short- and long-term forecasts of snow depth, J. Appl. Stat., 45, 1133–1156,
630   https://doi.org/10.1080/02664763.2017.1357683, 2018.

Hanzer, F., Helfricht, K., Marke, T., and Strasser, U.: Multilevel spatiotemporal validation of snow/ice mass balance and runoff modelling in glacierized catchments, The Cryosphere, 10, 1859–1881, https://doi.org/10.5194/tc-10-1859-2016, 2016.

Hanzer, F., Förster, K., Nemec, J., and Strasser, U.: Projected cryospheric and hydrological impacts of 21st century climate change in the Ötztal Alps (Austria) simulated using a physically based approach, Hydrol. Earth Syst. Sci., 22, 1593–1614,
635   https://doi.org/10.5194/hess-22-1593-2018, 2018.

Harley, T. A.: Nice weather for the time of year: the British obsession with the weather. In: Strauss, S., Orlove, B. (eds.): Weather, climate, culture. Berg, Oxford, pp. 103–120, 2003.

Hersbach, H., Bell, B., Berrisford, P., Hirahara, S., Horányi, A., Muñoz-Sabater, J., Nicolas, J., Peubey, C., Radu, R., Schepers, D., Simmons, A., Soci, C., Abdalla, S., Abellan, X., Balsamo, G., Bechtold, P., Biavati, G., Bidlot, J., Bonavita, M., Chiara,
640   G. D., Dahlgren, P., Dee, D., Diamantakis, M., Dragani, R., Flemming, J., Forbes, R., Fuentes, M., Geer, A., Haimberger, L., Healy, S., Hogan, R. J., Hólm, E., Janisková, M., Keeley, S., Laloyaux, P., Lopez, P., Lupu, C., Radnoti, G., Rosnay, P. de,

Rozum, I., Vamborg, F., Villaume, S., and Thépaut, J.-N.: The ERA5 global reanalysis, Q. J. Roy. Meteor. Soc., 146, 1999–2049, https://doi.org/10.1002/qj.3803, 2020.

Jin, J., Gao, X., Yang, Z.-L., Bales, R. C., Sorooshian, S., Dickinson, R. E., Sun, S. F., and Wu, G. X.: Comparative Analyses

645 of Physically Based Snowmelt Models for Climate Simulations, J. Climate, 12, 2643–2657, https://doi.org/:10.1175/1520-0442(1999)012<2643:CAOPBS>2.0.CO;2, 1999.

Jordan, R.: A one-dimensional temperature model for a snow cover: Technical documentation for SNTHERM 89, Tech. rep., Hanover, NH, 1991.

Kouki, K., Räisänen, P., Luojus, K., Luomaranta, A., and Riihelä, A.: Evaluation of Northern Hemisphere snow water

650 equivalent in CMIP6 models during 1982–2014, The Cryosphere, 16, 1007–1030, https://doi.org/10.5194/tc-16-1007-2022, 2022.

Kouki, K., Luojus, K., and Riihelä, A.: Evaluation of snow cover properties in ERA5 and ERA5-Land with several satellite-based datasets in the Northern Hemisphere in spring 1982–2018, The Cryosphere Discuss. [preprint], https://doi.org/10.5194/tc-2023-53, in review, 2023.

655 Krinner, G., Derksen, C., Essery, R., Flanner, M., Hagemann, S., Clark, M., Hall, A., Rott, H., Brutel-Vuilmet, C., Kim, H., Ménard, C. B., Mudryk, L., Thackeray, C., Wang, L., Arduini, G., Balsamo, G., Bartlett, P., Boike, J., Boone, A., Chéruy, F., Colin, J., Cuntz, M., Dai, Y., Decharme, B., Derry, J., Ducharne, A., Dutra, E., Fang, X., Fierz, C., Ghattas, J., Gusev, Y., Haverd, V., Kontu, A., Lafaysse, M., Law, R., Lawrence, D., Li, W., Marke, T., Marks, D., Ménégoz, M., Nasonova, O., Nitta, T., Niwano, M., Pomeroy, J., Raleigh, M. S., Schaedler, G., Semenov, V., Smirnova, T. G., Stacke, T., Strasser, U., Svenson,

660 S., Turkov, D., Wang, T., Wever, N., Yuan, H., Zhou, W., and Zhu, D.: ESM-SnowMIP: assessing snow models and quantifying snow-related climate feedbacks, Geosci. Model Dev., 11, 5027–5049, https://doi.org/10.5194/gmd-11-5027-2018, 2018.

Liu, L., Ma, Y., Menenti, M., Su, R., Yao, N., and Ma, W.: Improved parameterization of snow albedo in Noah coupled with Weather Research and Forecasting: applicability to snow estimates for the Tibetan Plateau, Hydrol. Earth Syst. Sci., 25, 4967–

665 4981, https://doi.org/10.5194/hess-25-4967-2021, 2021.

Lynch-Stieglitz, M.: The Development and Validation of a Simple Snow Model for the GISS GCM, J. Climate, 7, 1842–1855, https://doi.org/10.1175/1520-0442(1994)007<1842:TDAVOA>2.0.CO;2, 1994.

Mathew, J. K., Liu, M., and Bullock, D. M.: Impact of Weather on Shared Electric Scooter Utilization. In Proceedings of the 2019 IEEE Intelligent Transportation Systems Conference (ITSC), Auckland, New Zealand, 27–30 October 2019; IEEE:

670 Auckland, New Zealand, October 2019; pp. 4512–4516.

Matiu, M. and Hanzer, F.: Bias adjustment and downscaling of snow cover fraction projections from regional climate models using remote sensing for the European Alps, Hydrol. Earth Syst. Sci., 26, 3037–3054, https://doi.org/10.5194/hess-26-3037-2022, 2022.

Meyer, J., Kohn, I., Stahl, K., Hakala, K., Seibert, J., and Cannon, A. J.: Effects of univariate and multivariate bias correction

675   on hydrological impact projections in alpine catchments, Hydrol. Earth Syst. Sci., 23, 1339–1354, https://doi.org/10.5194/hess-23-1339-2019, 2019.

Moody, E. G., King, M. D., Schaaf, C. B., Hall, D. K., and Platnick, S.: Northern Hemisphere five-year average (2000–2004) spectral albedos of surfaces in the presence of snow: Statistics computed from Terra MODIS land products, Remote Sens. Environ., 111, 337–345, https://doi.org/10.1016/j.rse.2007.03.026, 2007.

680   Mooney, P. A., Rechid, D., Davin, E. L., Katragkou, E., de Noblet-Ducoudré, N., Breil, M., Cardoso, R. M., Daloz, A. S., Hoffmann, P., Lima, D. C. A., Meier, R., Soares, P. M. M., Sofiadis, G., Strada, S., Strandberg, G., Toelle, M. H., and Lund, M. T.: Land–atmosphere interactions in sub-polar and alpine climates in the CORDEX Flagship Pilot Study Land Use and Climate Across Scales (LUCAS) models – Part 2: The role of changing vegetation, The Cryosphere, 16, 1383–1397, https://doi.org/10.5194/tc-16-1383-2022, 2022.

685   Muñoz-Sabater, J., Dutra, E., Agustí-Panareda, A., Albergel, C., Arduini, G., Balsamo, G., Boussetta, S., Choulga, M., Harrigan, S., Hersbach, H., Martens, B., Miralles, D. G., Piles, M., Rodríguez-Fernández, N. J., Zsoter, E., Buontempo, C., and Thépaut, J.-N.: ERA5-Land: a state-of-the-art global reanalysis dataset for land applications, Earth Syst. Sci. Data, 13, 4349–4383, https://doi.org/10.5194/essd-13-4349-2021, 2021.

Musselman, K. N., Lehner, F., Ikeda, K., Clark, M. P., Prein, A. F., Liu, C., Barlage, M., and Rasmussen, R.: Projected

690   increases and shifts in rain-on-snow flood risk over western north america, Nat. Clim. Change, 8, 808–812, https://doi.org/10.1038/s41558-018-0236-4, 2018.

Niu, G.-Y. and Yang, Z.-L.: Effects of vegetation canopy processes on snow surface energy and mass balances, J. Geophys. Res.-Atmos., 109, D23111, https://doi.org/10.1029/2004JD004884, 2004.

Niu, G. Y., Yang, Z. L., Mitchell, K. E., Chen, F., Ek, M. B., Barlage, M., Kumar, A., Manning, K., Niyogi, D., Rosero, E.,

695   Tewari, M., and Xia, Y: The community Noah land surface model with multiparameterization options (Noah-MP): 1. Model description and evaluation with local-scale measurements, J. Geophys. Res.-Atmos., 116, D12109, https://doi.org/10.1029/2010JD015139, 2011.

Pham, T. V., Steger, C., Rockel, B., Keuler, K., Kirchner, I., Mertens, M., Rieger, D., Zängl, G., and Früh, B.: ICON in Climate Limited-area Mode (ICON release version 2.6.1): a new regional climate model, Geosci. Model Dev., 14, 985–1005,

700   https://doi.org/10.5194/gmd-14-985-2021, 2021.

Poschlod, B., Hodnebrog, Ø., Wood, R. R., Alterskjær, K., Ludwig, R., Myhre, G., and Sillmann, J.: Comparison and evaluation of statistical rainfall disaggregation and high-resolution dynamical downscaling over complex terrain, J. Hydrometeorol., 19, 1973–1982, https://doi.org/10.1175/JHM-D-18-0132.1, 2018.

Poschlod, B., Willkofer, F., and Ludwig, R.: Impact of climate change on the hydrological regimes in Bavaria, Water, 12,

705   1599, https://doi.org/10.3390/w12061599, 2020a.

The Cryosphere
Discussions

Open Access

EGU

Poschlod, B., Zscheischler, J., Wood, R., Sillmann, J., and Ludwig, R.: Climate Change Effects on hydrometeorological compound events over Southern Norway, Weather and Climate Extremes, 28, https://doi.org/10.1016/j.wace.2020.100253, 2020b.

Quante, L., Willner, S. N., Middelanis, R., and Levermann, A.: Regions of intensification of extreme snowfall under future
710 warming, Sci. Rep., 11(1), 1–9, https://doi.org/10.1038/s41598-021-95979-4, 2021.

Räisänen, J.: Snow conditions in northern Europe: the dynamics of interannual variability versus projected long-term change, The Cryosphere, 15, 1677–1696, https://doi.org/10.5194/tc-15-1677-2021, 2021.

Richter, D.: Ergebnisse methodischer Untersuchungen zur Korrektur des systematischen Meßfehlers des Hellmann-Niederschlagsmessers, Tech. Rep., Deutscher Wetterdienst, Offenbach a. M., Germany, 1995.

715 Qi, W., Feng, L., Liu, J., and Yang, H.: Snow as an important natural reservoir for runoff and soil moisture in Northeast China, J. Geophys. Res.-Atmos., 125, e2020JD033086, https://doi.org/10.1029/2020jd033086, 2020.

Rybka, H., Haller, M., Brienen, S., Brauch, J., Früh, B., Junghänel, T., Lengfeld, K., Walter, A., and Winterrath, T.: Convection-permitting climate simulations with COSMO-CLM for Germany: Analysis of present and future daily and sub-daily extreme precipitation, Meteorol. Z. (Contrib. Atm. Sci.), 32, 2, 91–111, https://doi.org/10.1127/metz/2022/1147, 2022.

720 Saigger, M., Mölg, T., Schmid, C., and Sauter, T.: Simulating snow drift in WRF – First results and future plans of a novel module, EGU General Assembly 2023, Vienna, Austria, 24–28 Apr 2023, EGU23-12384, https://doi.org/10.5194/egusphere-egu23-12384, 2023.

Sasai, T., Kawase, H., Kanno, Y., Yamaguchi, J., Sugimoto, S., Yamazaki, T., Sasaki, H., Fujita, M., and Iwasaki, T.: Future projection of extreme heavy snowfall events with a 5-km large ensemble regional climate simulation, J. Geophys. Res. Atmos.,
725 124, 13975–13990, https://doi.org/10.1029/2019JD030781, 2019.

Schaaf, C. and Wang, Z.: MODIS/Terra+Aqua BRDF/Albedo Albedo Daily L3 Global 0.05Deg CMG V061 [data set], NASA EOSDIS Land Processes DAAC, https://doi.org/10.5067/MODIS/MCD43C3.061, 2021.

Schulz, J.-P. and Vogel, G.: Improving the Processes in the Land Surface Scheme TERRA: Bare Soil Evaporation and Skin Temperature, Atmosphere, 11, 5, https://doi.org/10.3390/atmos11050513, 2020.

730 Schulz, J.-P., Vogel, G., Becker, C., Kothe, S., Rummel, U., and Ahrens, B.: Evaluation of the ground heat flux simulated by a multi-layer land surface scheme using high-quality observations at grass land and bare soil, Meteorol. Z., 25, 607–620, https://doi.org/10.1127/metz/2016/0537, 2016.

Simpkins, G.: Snow-related water woes, Nat. Clim. Change, 8, 945, https://doi.org/10.1038/s41558-018-0330-7, 2018.

Skamarock, C., Klemp, B., Dudhia, J., Gill, O., Liu, Z., Berner, J., Wang, W., Powers, G., Duda, G., Barker, D., and Huang,
735 X.-Y.: A Description of the Advanced Research WRF Model Version 4, NCAR, Boulder, Colorado, USA, https://doi.org/10.5065/1dfh-6p97, 2019.

Slatyer, R. A., Umbers, K. D. L., and Arnold, P. A.: Ecological responses to variation in seasonal snow cover, Conserv. Biol., 36, e13727, https://doi.org/10.1111/cobi.13727, 2022.

Sørland, S. L., Brogli, R., Pothapakula, P. K., Russo, E., Van de Walle, J., Ahrens, B., Anders, I., Bucchignani, E., Davin, E.
740 L., Demory, M.-E., Dosio, A., Feldmann, H., Früh, B., Geyer, B., Keuler, K., Lee, D., Li, D., van Lipzig, N. P. M., Min, S.-
K., Panitz, H.-J., Rockel, B., Schär, C., Steger, C., and Thiery, W.: COSMO-CLM regional climate simulations in the
Coordinated Regional Climate Downscaling Experiment (CORDEX) framework: a review, Geosci. Model Dev., 14, 5125–
5154, https://doi.org/10.5194/gmd-14-5125-2021, 2021.

Steiger, R., Scott, D., Abegg, B., Pons, M., and Aall, C.: A critical review of climate change risk for ski tourism, Curr. Issues
745 Tour., 1–37, https://doi.org/10.1080/13683500.2017.1410110, 2017.

Strasser, U.: Snow loads in a changing climate: new risks?, Nat. Hazards Earth Syst. Sci., 8, 1–8, https://doi.org/10.5194/nhess-
8-1-2008, 2008a.

Strasser, U.: Modelling of the mountain snow cover in the Berchtesgaden National Park, Tech. Rep. 55, Berchtesgaden
National Park, Berchtesgaden, 2008b.

750 Sun, S., Jin, J., and Xue, Y.: A simple snow-atmosphere-soil transfer (SAST) model, J. Geophys. Res., 55, 1206–1216,
https://doi.org/10.1007/s11430-011-4328-5, 1999.

Taszarek, M., Kendzierski, S., and Pilguj, N.: Hazardous weather affecting European airports: Climatological estimates of
situations with limited visibility, thunderstorm, low-level wind shear and snowfall from ERA5, Weather and Climate Extremes,
28, 100243, https://doi.org/10.1016/j.wace.2020.100243, 2020.

755 Tomasi, E., Giovannini, L., Zardi, D., and de Franceschi, M.: Optimization of Noah and Noah_MP WRF land surface schemes
in snow-melting conditions over complex terrain, Mon. Weather Rev., 145, 4727–4745, https://doi.org/10.1175/MWR-D-16-
0408.1, 2017.

Trinks, C., Hiete, M., Comes, T., and Schultmann, F.: Extreme weather events and road and rail transportation in Germany,
Int. J. Emerg. Manag., 8, 207–227, https://doi.org/10.1504/IJEM.2012.047525, 2012.

760 Verseghy, D. L.: Class – A Canadian land surface scheme for GCMS. I. Soil model, Int. J. Climatol., 11, 111–133,
https://doi.org/10.1002/joc.3370110202, 1991.

Warren, S. G.: Optical properties of ice and snow, Philos. Trans. A Math. Phys. Eng. Sci., 377, 20180161,
https://doi.org/10.1098/rsta.2018.0161, 2019.

Warscher, M., Wagner, S., Marke, T., Laux, P., Smiatek, G., Strasser, U., and Kunstmann, H.: A 5 km Resolution Regional
765 Climate Simulation for Central Europe: Performance in High Mountain Areas and Seasonal, Regional and Elevation-
Dependent Variations, Atmosphere, 10, 682, https://doi.org/10.3390/atmos10110682, 2019.

Warscher, M., Hanzer, F., Becker, C., and Strasser, U.: Monitoring snow processes in the Ötztal Alps (Austria) and
development of an open source snow model framework, EGU General Assembly 2021, online, 19–30 Apr 2021, EGU21-9101,
https://doi.org/10.5194/egusphere-egu21-9101, 2021.

770 Winter, K. J. P. M., Kotlarski, S., Scherrer, S. C., and Schär, C.: The Alpine snow-albedo feedback in regional climate models,
Clim. Dyn., 48, 1109–1124, https://doi.org/10.1007/s00382-016-3130-7, 2017.

Witting, M. and Schmude, J.: Impacts of climate and demographic change on future skier demand and its economic consequences—Evidence from a ski resort in the German alps, J. Outdoor Recreat. Tour., 26, 50–60, https://doi.org/10.1016/j.jort.2019.03.002, 2019.

775 Xue, Y., Sun, S., Kahan, D. S., and Jiao, Y.: Impact of parameterizations in snow physics and interface processes on the simulation of snow cover and runoff at several cold region sites, J. Geophys. Res., 108, https://doi.org/10.1029/2002JD003174, 2003.

Yang, H., Xie, K., Ozbay, K., Ma, Y., and Wang, Z.: Use of Deep Learning to Predict Daily Usage of Bike Sharing Systems, Transp. Res. Rec. J. Transp. Res. Board, 2672, 92–102, https://doi.org/10.1177/0361198118801354, 2018.

780